LUT University
LUT School of Energy Systems
Energy Technology

Henry Vesalainen

Approaches to the thermal analysis of ship-based LNG tanks under harsh external environmental conditions

16.08.2021

Examiners: Professor, D.Sc Teemu Turunen-Saaresti
M.Eng. Rob Hindley

ABSTRACT

LUT University
LUT School of Energy Systems
LUT Energy Technology

Henry Vesalainen

Approaches to the thermal analysis of ship-based LNG tanks under harsh external environmental conditions

Master’s thesis

2021

66 Pages, 24 figures, 9 tables, and 4 appendices

Examiners: Professor, D.Sc Teemu Turunen-Saaresti
M.Eng. Rob Hindley

Keywords: LNG carrier, membrane tank, temperature distribution of hull structure

This thesis investigates the usability of CFD modeling in LNG carrier hull thermal design. The study focuses on the membrane type of tank that is the most common tank-type in carrying LNG nowadays. Carrying LNG along the arctic sea roads exposes the hull structures to extreme cold temperatures because the heat flux through the tank structure is minor. The situation could be seen as an advantage from BOG's point of view but an increased challenge from the hull durability point of view. For fulfilling the requisites of hull steel parts, the thermal analysis must execute. In this way, the ship's safety operation is ensured, and the material cost in the construction phase is optimized. The main aim of this thesis is to execute thermal analysis for the carrier’s steel structure.

IMO’s IGC code is a driving force in LNG carriers' design. It can be stated that the IMO’s regulations are not given practical help for designers. The more specific guidelines are established from classification societies, and these guidelines are helping the designer to achieve the requirements.

The main part of the thesis states that executing manual 1-D calculations is a good way to achieve the calculation boundaries for the CFD model. The results from the CFD simulations are reasonable and coherent with manual calculations. The used mesh resolutions did not show a significant effect on temperature distributions of the inner hull. Based on the results, the steel grade design could be executed by using these modeling tools. CFD calculations were executed with ANSYS student license.

TIIVISTELMÄ

LUT-Yliopisto
LUT Shcool of Energy Systems
LUT Energiatekniikka

Henry Vesalainen

Approaches to the thermal analysis of ship-based LNG tanks under harsh external environmental conditions

Diplomityö

2021

66 sivua, 24 kuvaa, 9 taulukkoa and 4 liitettä

Tarkastajat: Professori, TkT Teemu Turunen-Saaresti
M.Eng Rob Hindley

Hakusanat: LNG tankkeri, membraani tankki, rungon lämpötilajakauma

Tässä diplomityössä kartoitetaan numeerisen virtausdynamiikan käytettävyyttä LNG tankkerin rungon rakenteen lämpötilajakauman määrittämiseksi. Tutkimuksessa keskitytään membraani tyypin tankkiin, joka on nykypäivänä käytetyin eristystapa LNG:n kuljetuksessa. LNG:n kuljetus läpi arktisten alueiden altistaa rungon rakenteita erittäin kylmille lämpötiloille, koska lämpövirta ympäristöstä rungon rakenteisiin on vähäistä. Tämä voidaan nähdä selkeänä etuna syntyvän höyrystymishävikin kannalta, mutta haasteena terästen lämpötilasuunnittelussa. Jotta vaatimukset iskusitkeyden kannalta täyttyvät erittäin kylmänkin ympäristön lämpötiloissa, täytyy rungon rakenteelle tehdä kattavaa lämpötila-analyysi. Tällä turvataan aluksen turvallinen toiminta, sekä tehostetaan rakennusvaiheen materiaalikustannuksia. Diplomityön tavoite on tehdä LNG kuljetusaluksen teräsrakenteelle lämpötila-analyysi.

Työn alussa käydään läpi LNG-tankkereiden runkojen teräsrakenteiden kansainvälistä sääntelyä ja todetaan IMO:n säätelevän suunnittelun isoimpia suuntaviivoja, mutta luokittelulaitosten ohjaus on huomattavasti tarkempaa laivansuunnittelijan näkökulmasta.

Tutkimusosiossa todetaan manuaalisten laskujen olevan oivallinen tapa löytää sopivat yksinkertaistukset CFD-mallin rakentamiseen. Ansys-opiskelijalisenssillä onnistuttiin mallintamaan realistinen lämpötilajakauma tankkerin rungolle. Mallinnetut lämpötilajakaumat olivat koherentteja manuaalisesti laskujen kanssa. Tutkimuksessa käytetyillä menetelmillä voitaisiin määrittää tarvittavat teräslaadut aluksen rungolle.

ACKNOWLEDGEMENTS

Five years in Lappeenranta went fast. That being said, I am heading forward with many unforgettable memories. I am glad for the people whom I got to know during the wonderful journey. Therefore, I would like to show my appreciation, and tell how thankful I am of this. Thank you Atte, Tommi, and especially Kasperi, for all the help during my studies. I learned a lot with you guys. We always liked to do high-quality work with proper touch, but never with too serious-minded.

I want to thank the LUT-university community. It was always nice to go to the campus. LUT's spirit is warm, and the scientific community is hungry. Many professors and lecturers have an enthusiastic attitude toward the topics that they are teaching. Thanks to Dr. Teemu Turunen-Saaresti for guiding my Diploma Thesis. The guidance you gave me was the key to get this project done.

I would like to thank Aker Arctic Technology Inc & Rob Hindley for making this thesis project possible. I also want to thank Esa Hakanen for sharing his knowledge related to arctic ship design.

In the end, I want to thank my family. Thanks mom, that you have always supported me. Thanks Dad, for encouraging me to accomplish an academic degree. Also, thank you my darling for taking care of our newborn daughter during this thesis.

Henry Vesalainen

16.08.2021 Vantaa

TABLE OF CONTENT

SYMBOLS AND ABBREVIATIONS

Latin alphabet

A	Area	m^2
E	Energy	J
g	Gravity	kg/ms^2
h	Convection heat transfer coefficient	W/m^2K
H/L	Aspect ratio	-
k	Conductivity	W/mK
L	Characteristic length	mm,m
Q, q	Heat flux	W/m^2
T	Temperature	K, °C
t	Thickness	mm,m
U	Overall heat transfer coefficient	W/m^2K
u	Velocity	m/s

Greek alphabet

α	Thermal diffusivity	m^2/s
β	Thermal expansion coefficient	1/K
Δ	Difference	-
ε	Emissivity	-
μ	Kinematic viscosity	kg/sm, Ns/m^2
ν	Dynamic viscosity	m^2/s
ρ	Density	kg/m^3
σ	Stefan-Boltzmann-constant	W/m^2K^4

Dimensionless numbers

Gr	Grashof number
Nu	Nusselt number
Pr	Prandtl number
Ra	Rayleigh number
Re	Reynolds number
$y+$	Dimensionless wall distance

Subscripts

∞	Environment
CO	Compartment
cond	Conduction
conv, c	Convection
IH	Inner hull
INS	Insulation

m,n	Nodal point’s x & y coordinates
OH	Outer hull
rad	Radiation
tot	Total
s	Surface

Abbreviations

1-D	1-Dimensional
2-D	2-Dimensional
3-D	3-Dimensional
BOG	Boil-off gas
BOR	Boil-off rate
CCS	Cargo Containment System
CFD	Computational Fluid Dynamics
DNV	Det Norske Veritas, classification society
GTT	Gaztransport & Technigaz
IACS	International Association of Classification Socitities
IGC Code	International Gas Carrier Code
IMO	International Maritime Organization
KR	Korean Register, classification society
LNG	Liquefied Natural
LR	Lloyd’s Register, classification society
Mark III	GTT’s insulation system
NO-96	GTT’s insulation system
USCG	United States Coast Guard

1 INTRODUCTION

Global warming and the development of LNG (Liquefied Natural Gas) shipping have connived the availability of natural resources and the use of arctic sea roads (Pastusiak 2016, pp. 3). The need for the transportation of LNG through external harsh environmental conditions is increased (Mokhtatab 2014, pp. 21). The external low operation temperatures and effect of ice cause requirements for the ship design.

The LNG carrying ships' design is strongly guided by international rules and regulations, which specify requirements for safety aspects for the ship design. The most important regulations related to this thesis work are focusing on the used steel grades around the tank. Especially when the designed ship operates in a low-temperature environment, LNG tanks' surroundings might face low temperatures. The ship structure faces LNG's cold temperature from inside the ship and cold temperature from the environment. This leads to a need for the use of high-quality and expensive steel grades. If the thermal analysis for the hull structure can be done reliably, it leads to the ship's safe operation and material savings in the ship's construction phase.

This thesis work investigates the heat transfer phenomena around the LNG carrier's membrane tanks. The study focuses on ice-going LNG carriers that are facing harsh external environmental conditions during their operation. The thesis examines which heat transfer phenomena are most relevant to consider while calculating and determining the temperatures for the steel grades on ship structure and which heat transfer phenomena are less relevant. The main aim is to find the most efficient and reliable ways to do the thermal analysis for the ship hull.

As history has shown in the worst-case scenario, if the LNG carrier hull structure occurs thermal stress, the ship operation is highly endangered (IMO, 2007, pp. 54-81). That is the reason why thermal stress analysis should not be underestimated during the ship design phase, especially when the designed ship will operate in the arctic region where it might face extremely cold ambient conditions.

1.1 Background

This thesis work is supported by a ship design company Aker Arctic Technology Inc. Aker Arctic is a Finnish ship design company specialized in the concept and preliminary phase design for ice-going ships. The company is motivated to take part in this thesis work because they are willing to improve their knowledge of the thermal analysis part of the LNG carrier design process. They are working in the small ship design field, where scientific information is tricky to find from the public research field. This leads to the situation where they have to and are willing to do many studies during the projects. Aker Arctic Technology can be seen as one of the forerunners of the arctic ship design field.

The ships on this artic segment are facing many kinds of environmental conditions. The varying operation temperatures cause challenges for the decision of design temperatures and steel grades. The temperatures of the worst-case scenario are determining the needed steel grades for the ship's construction. The baselines for the calculations of the temperature distribution of the hull structure are following the IMO's (International Maritime Organization) codes and classification societies' guidelines. The challenges show up when the ship is designed to operate even lower ambient temperature conditions what the IMO's regulations are straightly guiding.

Using numerical simulation as a solving tool for LNG industrial problems has become more popular. Regarding many scientific studies related to the LNG carries, the use of CFD (computational fluid dynamics) models can be a relevant tool for achieving accurate thermal analysis results. That is why the company is interested in knowing the possibilities of CFD for making thermal analyses.

Using CFD software as a tool requires a good knowledge of numerical methods, fluid dynamics, and heat transfer theory. My background faces the requirements of this study, so it was easy to find common ground with Aker Arctic.

1.2 Objectives and study questions

This thesis's main objective is to find reliable, accurate, and practical design tools to execute thermal analysis for the ship-based LNG membrane tanks' surrounding

structures. This includes the investigation of the pros and cons of manual and CFD-based calculations for the thermal distribution on the ship's hull structure.

The research aims to determine the temperature distribution on structures during the ship's normal operation. The study questions of the research can be seen below.

1. How the heat transfer phenomena behave, and what influences the temperatures on steel structures?
2. How should the temperatures in the steel structure be determined?
3. How useable is the CFD software usage in the determination of LNG carrier's hull structure temperature distribution? What does it take to achieve reliable results?
4. How to face the LNG leakage situation?

1.3 Scope of the research

The main focus is to overview the different possibilities to execute the thermal design for the LNG carrier tank's surrounding structure. The LNG carrier used as an example in the research has a capacity of around 150 000 $m^{3,}$ and has a membrane-type tank. The thermal design is primarily executed using the cross-section of the midship section. The study follows international rules and regulations, which are reviewed in chapter 2.1 Regulations and guidelines. Rules and regulations are overviewed insofar as it is relevant.

1.4 Hypothesis and benefits of research

It is expected that the thermal design of the LNG carrier can be done by manual calculations and as well by the numerical solution-based CFD software. It is expected that the approximate results can be achieved both ways, but determining precisely the local thermal stresses is expected to be more effortless to achieve by using CFD software. Determining exactly local thermal stresses in hull structure is expected to be complicated by the manual way because the number of equations increases when phenomena want to be executed in the 2-D (2-Dimensional) or 3-D (3-Dimensional).

It is expected to find out which heat transfer phenomena have a major effect on the analysis. The convection and conduction effects of the total share of the heat transfer are

expected to be greater than the share of radiations because investigated heat transfer problem consists of certainly low temperature and temperature differences (Incropera, et al., 2007, p. 9; Ding, et al., 2010, p. 348). Implementations of the 1-D (1-Dimensional) models are expected to be undoubtedly easy to execute by manual calculations because the classification societies are providing quite clear guidance for that (American Bureau of shipping, 2019). The 2-D and 3-D models where the wind effect and water movement could be taken into account more realistic are expected to be more complicated to execute. The number of terms increases in the multidimensional models, leading to an even more complicated situation, and building a useful tool is even more challenging.

The multidimensional models might occur challenges with computing power demand while using CFD tools. It is expected that the wind and water movement have minor effects on the results, but it is assumed that they have still more significant effection than radiation. It is expected that the effect of radiation is the least effecting because of small temperatures and temperature differences (Incropera, et al., 2007, pp. 9-11).

Additionally, there are expected findings on how fast the critical temperatures in the hull structure are achieved when the tank's secondary barrier is damaged. Tank structure is explained more precisely in chapter 2.2.1 Cargo containment systems. The precautionary concepts are overviewed for the leakage situation, but there are assumed to be difficulties finding enough reliable findings for the solutions that could be technically and economically implemented, except for the cofferdam area.

If the study executes the thermal analysis for hull structure successfully, the research gives designers trustable options to execute thermal design as the rules and regulations are expecting. As well the study is determining how to do the thermal design time-effectively.

1.5 Literature review

The research field around the LNG carriers is active. Most of the research papers are focusing on the CCS (Cargo containment system) systems' insulation capability and develop it. Also, the determination of the amount of BOG (Boil-off Gas) is a hot research topic. The effective insulation and the amount of BOG are going hand in hand.

Choi, et al. (2012) studied the capabilities of two well-known insulation systems. The bullet point from the research was that both popular insulation systems have approximately the same capability to resist heat transfer, and the heat is resisted linearly through to insulation structure. They also included the LNG leakage scenario in their research paper. Sung, Han & Woo (2016) also studied the leaked LNG thermal effect for safety in LNG CCS. Their study's main point was to determine if the leakage occurs how fast the crack size and the mass flow of the leakage exposes the structure at critical temperatures. Ding, Tang & Zhang (2010) also studied the thermal stress at a general level and with incomplete insulation. They concluded that the key to simulate the temperature field successfully is to optimize calculation parameters for the convection between the inner and outer hull.

Joeng and Shim (2017) explored the possibilities of new insulation structure capabilities usage in LNG carriers. The Koreans have innovated the new insulation structure, which tries to compete against the traditional double layer-based products. Preliminary results seem promising.

These mentioned studies have applied the CFD as a tool of their study, and this gives a good manner for that the CFD could be potentially applied successfully in this thesis as well. Also, free convection modeling with CFD has been studied in many research papers example, Boz, Erdogdu & Tutar (2014) investigated how mesh refining affects free convection modeling. They stated that the mesh refining will not always affect to the results of free-convection applications. This thesis study includes free-convection areas, so it will be interesting to see how their results will face this thesis results that come to the mesh refining.

A couple of the used references, their key findings, and where the information were applied on this thesis can be found in Table 1.

Table 1 Couple of references which were used during this thesis.

Author & Year	Key findings	Applied on this study
(Boz, et al., 2014)	• Mesh refinement effect to the free convection modeling	• Considered during the mesh building
(Choi, et al., 2012)	• Thermal properties of two main insulation systems • How the leakage occurs	• Insulation system thermal properties were used in calculations
(Joeng & Shim, 2017)	• BOG amount • Temperature distribution on steel structure	• Temperature distributions were compared to the calculation results

2 LNG CARRIERS DESIGN

This chapter is going through the regulations and guidelines that drive the LNG carriers' design. Also, the ship's basic geometry and typical insulation structures of membrane tanks are overviewed.

2.1 Regulations and guidelines

This chapter overviews the international regulations related to the LNG carrier's design from the structure thermal design points of view. The root cause for doing the thermal analysis is to make sure that the structure lasts under the influence of temperature stresses. Regulations are guiding the steel grade selection based on design temperatures. Designing LNG carriers to the polar waters and following the guidelines is not always so easy and unambiguous.

2.1.1 International Maritime Organization

IMO is the main decisive body of the marine field. All the baselines for design, operation, legal matters, and emission comes from the IMO. For this thesis, the Code for the Construction and Equipment of Ships Carrying Liquefied Gases in Bulk, IGC Code, is the most relevant regulation document related to the LNG carriers' design. The IGC code gives the main design parameters for LNG carriers' design process. All the mainlines that are related to the ship structure, LNG safety carrying, and operation are determined in this code. (IMO, 2014)

The most relevant chapters of the code are Chapter 02, 03, 04, 06, 07, and 18 from the thermal design point of view. Chapter 2.4 of the IGC code specifies the location of cargo tanks (IMO, 2014, pp. 20-26). Chapter 3.1 of the IGC code specifies requirements for the segregation of the cargo area (IMO, 2014, p. 32). Chapter 04 handles the cargo containments (IMO, 2014, pp. 41-71). Chapters 2.4 and 3.1 of the IGC code are important to understand because the structure is built up based on these chapters and determines geometry for the calculation. Chapter 04 of the IGC code includes essential information and requirements about the membrane tank and its insulation, materials, and structure. These are important to understanding the entity. Also, if the leakage situation is investigated, there should be considered the 15 days safety period requirements. If the

secondary barrier faces a leakage situation, the insulation system should handle it for at least 15 days without risking ship safety (IMO, 2014, pp. 44-45).

Chapter 06 determines the materials of construction. The most important section is table 6.5 of the code, which can be seen in Table 2. The table determines typical steel grades for the construction and guides the temperature scale when they should be used. The markable notice concerning this research is that sometimes the design temperatures of ship hull parts are below -30°C, then the table doesn't give any more help to the designers. The code says that below -30 °C, the hull material choice has to be based on Table 6.2 of the code. From table 6.2 can be found guidance for the construction down to -55 °C design temperature. In the external harsh environmental conditions, there might form even colder temperatures than -55°C in some local spots of the hull structure. The response of the IGC code is to move on to table 6.3. Table 6.3 of the code reaches design temperature down to -165 °C. Tables 6.2 and 6.3 are a bit problematic from a hull structure point of view. They are not providing any specific steel grades. They focus on guiding the composition of the steel grade. Used steel grade should stand the thermal and the mechanical stress targeted at the ship hull during winter navigation. The tables 6.2 and 6.3 can be found in Appendix I and Appendix II. (IMO, 2014, pp. 91-102).

Table 2 Plates and sections for hull structures according to ICG CODE (IMO, 2014, p. 102).

PLATES AND SECTIONS FOR HULL STRUCTURES REQUIRED BY 4.19.1.2 AND 4.19.1.3							
Minimum design temperature of hull structure (°C)	Maximum thickness (mm) for steel-grades						
	A	B	C	E	AH	DH	EH
0 and above[See note 1] -5 and above[See note 2]	Recognized standards						
down to -5	15	25	30	50	25	45	50
down to -10	x	20	25	50	20	40	50
down to -20	x	x	20	50	x	30	50
down to -30	x	x	x	40	x	20	40
Below -30	In accordance with table 6.2, except that the thickness limitation given in table 6.2 and in note 2 of that able does not apply.						
Notes "x" means steel grade not to be used 1 For the purpose of 4.19.1.3. 2 For the purpose of 4.19.1.2.							

The steel grade selection is shown more clarified on the classification societies' guidelines when the structure temperatures are going below -30°C.

Chapter 07 of the IGC code determines in section 7.2 the upper ambient design temperature for the sea at 32°C and air at 45°C (IMO, 2014, p. 108). And these are the conditions where the tanks' manufacturers typically present the BOG values for the membrane system. Chapter 18.5 of the code sets requirements for carriage at low temperature, and it says that the designed hull structure's temperatures should not fall below which the material cannot stand (IMO, 2014, p. 159).

As we can see, there are no straightforward guidelines available from IMO's IGC code on how the thermal analysis should be done, but still, it gives the baselines and boundaries of why it should be done. The main reason is to ensure the safety of the ship structure.

2.1.2 U.S. Coast Guard (USCG)

Although the U.S. Standards are mainly targeted to the U.S. flag state ships, some design requirements have become established internationally. The settled requirements for LNG carriers mainly follow the IGC code, but some additional requirements for cargo and its surrounding areas are related to arctic design. USCG requires to decrease the ambient design temperature to LNG carriers design to -29°C for air temperature and -2°C for seawater in Alaska, and excluding Alaska -18°C and 0°C (USCG, 2015, p. 42). Especially design values used in Alaska are usually used as a baseline around the world for LNG carriers in the arctic region.

2.1.3 Classification societies

Classification organizations have a significant part in guiding ships' design. The main aims of the classification companies are to classify and inspect ships, but they also conclude some researches, technical standards, and guidelines to the related design requirements. Technical rules and guidelines are based on experimental knowledge from the past and the best available information from current research. The main aim of the documents is to confirm that designs are meeting international requirements. Classification societies' policies are always done according to the IMO's policy. More

than 90% of the classification societies are members of IACS (International Association of Classification Societies) (IACS, 2021).

It is relevant to overview some of the classification societies and their rules and regulations because they are giving more specific information for the thermal design process. The content between the different classification societies is mainly the same. At least between the most prominent classification societies. The classification societies are doing reports on how to fulfill the requirements according to IMO's codes. Usually, the report structure follows the IMO code rationally, but they have expanded the content to be more specific. Also, classification societies have guidelines for topics that are not directly handled in the IMO's codes. Classification societies produce guidelines on how to do thermal analyses for LNG carriers. While taking a look at these guidelines, there can be found essential aspects for the designers who are executing the LNG carriers' thermal design.

Example LR (Lloyd's Register) and KR (Korean Register) have published their guidelines related to the LNG carriers thermal design: *Guidelines for Requirements of Thermal Analysis for the Hull Structure of Ships Carrying Liquefied Gases in Bulk* and *Guidance of Heat Transfer Analysis for Ships Carrying Liquefied Gases in Bulk/Ships using liquefied gases as fuels* (Lloyd's Register, 2016; Korean Register, 2020). These documents consist of more specific information on how the heat transfer phenomena have to be considered in the design process and how it should be executed. Both documents are approaching the topic from a bit different angle but targeting the same goal. Other classification societies provide the same type of guidelines, where the content is mainly the same.

LR's guideline document includes general information about different tank types, the basic theory of the models, and assumptions for the model building (Lloyd's Register, 2016). The report holds the minimum knowledge what designer have to know and understand when he or she is planning to start the thermal design process. In turn, the KR's guideline document is mathematically much more informative. It includes almost all necessary instruments for the manual calculation execution and the essential initial values for building a CFD-based solver (Korean Register, 2020). One important table can be found from both guidelines. The table consists of ambient conditions, and these are

internationally established values for the design. The table shows air temperature, seawater temperature, and wind speed according to IGC code and USCG safety standards, and it is presented in Table 3.

Table 3 Ambient conditions for temperature distribution calculations according to IGC and USCG (Korean Register, 2020, p. 15; Lloyd's Register, 2016, p. 2).

Regulation	Air Temperature [°C]	Seawater Temperature [°C]	Wind speed [knots]
ICG code	5	0	0
IGC code, warm condition	45	32	0
USCG, excluding Alaska	-18	0	5
USCG, including Alaska	-29	-2	5

These listed conditions give good fundaments to design, but even the USCG's Alaska conditions might be deficient in some cases. In that case, the ambient conditions have to be based on experimental knowledge and the best valid data that is available. Typically the end-user has the final word for the decision of the design temperature. Classification societies might also have their own guidelines for the external harsh conditions. These documents are primarily focusing on the ships that are designed to operate in the arctic conditions. What comes to the design temperatures example in the DNV's (Den Norske Veritas) *Winterization for climate operations* document guides that in Polar water should be used -45°C for ambient air and -2°C for seawater (DNV·GL, 2015, p. 81). The usage of the right design temperature generally ensures the hull endurance and adequate heating capacity in the ship.

2.2 LNG carrier structure

LNG carrier cargo section structure can be seen in Figure 1. As we can see, the holding structure is the ship's double hull. The tank membrane system also has a double structure. The double hull structure in the bottom and sides is also working as a ballast tank. The trunk deck has an important role in the arctic LNG carriers. It is a heated and insulated space and enables piping routing via cargo area in a weather protected location. The typical location of it can be seen in Figure 1. The piping's require plus degrees to avoid the fluid from freezing. Usually, the trunk deck has a walkway for maintenance service, and the piping goes under, and beside the walkway. The hull bottom typically has at least one pipe duct, and it is usually located in the middle of the hull. (Mokhatab, et al., 2013, p. 15).

From the thermal design point of view, it is important to ensure that the membrane structure is complying with the inner hull (Sung, et al., 2016, p. 278). Also, the heating capacity of the trunk deck has to be sufficient, so it is sure that the piping's are not freezing under any environmental conditions. Most important is to make sure that the hull steel grade selections last all mechanical and thermal stresses.

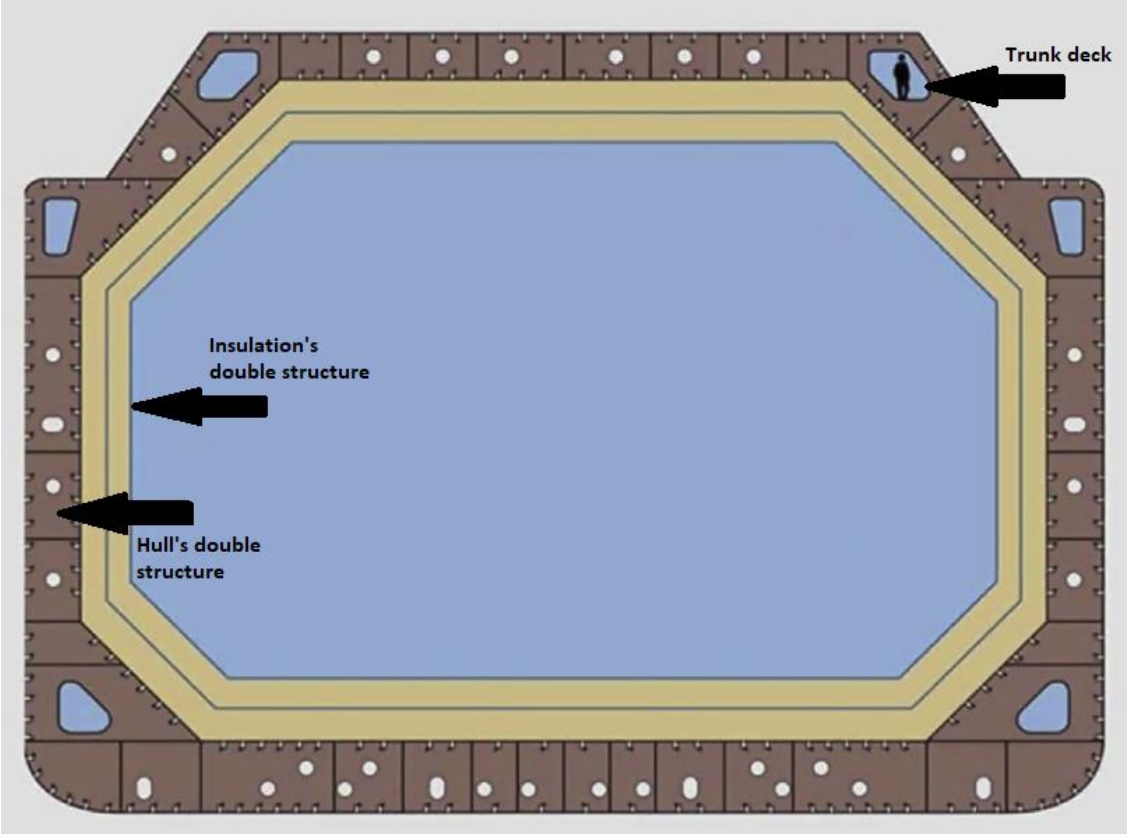

Figure 1 Principal schema of LNG carrier midsection structure (Mokhatab, et al., 2013, p. 15)

2.2.1 **Cargo containment systems**

CCS's (Cargo containment system) structure and insulation the main function is to keep transported LNG cold during transportation. The main goal is to do it as efficiently as possible and thus minimize the forming of BOG (Boil-off Gas). The membrane system is also protecting the surrounding areas from extremely cold temperatures. The two major types of membrane tanks on the global markets are Mark-III and NO-96 for LNG transporting. Both membrane types have a double structure. The double insulation structure ensures system redundancy in case of leakage. (Sung, et al., 2016, p. 278)

NO 96 system is made of two metallic membranes and two insulation layers. Both membranes are made from invar, a 36% nickel-steel alloy, by 0.7 mm thickness. Primary and secondary insulation materials are typically made from expanded perlite. In more advanced models, the insulation material can be glass-wool or a mix of glass-wool and foam, depending on the tank model. Insulation modules are supported with plywood boxes. Primary insulation box thickness is typically 230 mm, and secondary insulation box thickness is 300mm. Primary insulation layer thickness can be adjusted to face the desired amount of BOG. Overall, the structure is built that way if the leakage happens, the cold LNG can spread only in one section of the insulation structure. NO96 system can be seen in Figure 2. (GTT, 2020b)

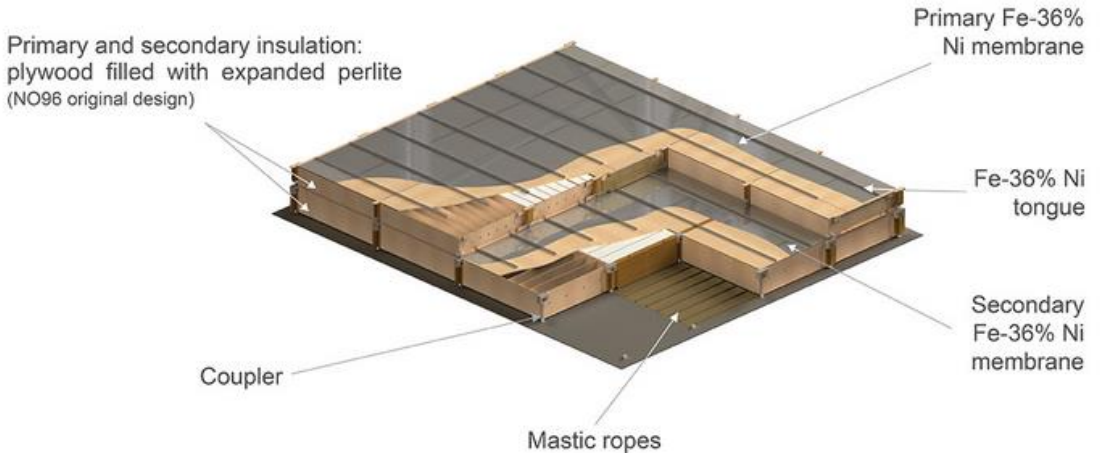

Figure 2 Visualized NO96 structure (GTT, 2020b).

GTT promises the BOR (Boil-off Rate) from 0.15% to 0.10% for 170 000 m^3 vessel, depending on the NO96 tank model. The amount of the BOG on is represented in the IGC code warm conditions. (GTT, 2020b)

Mark III systems' primary barrier is made from stainless steel 304L, and its thickness is 1.2mm. Secondary barriers are made from Triplex composite material. The panels' main insulation material is foam, and it is supported by plywood. Primary insulation panels have 100mm thickness, and secondary panels are from 170mm to 380mm depending on the membrane system-specific model. NO96 system can be seen in Figure 3. (GTT, 2020a)

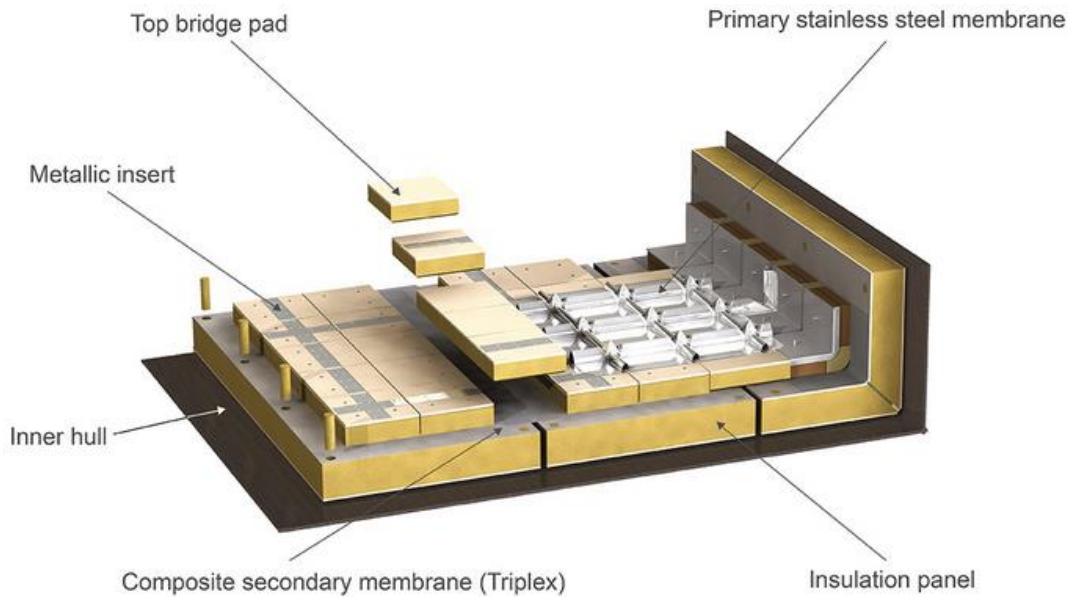

Figure 3 Visualized Mark III structure (GTT, 2020a).

GTT promises BOR from 0.15% to 0.07% for the 170 000 m^3 vessels with Mark III insulation systems (GTT, 2020a).

Comparing the Mark III structure to the NO 96 structure most significant difference is that the Mark structure is panel-based. In turn, the NO 69 system is box-based. The decision of the membrane system selection depends on a case by case. The aspects that are affecting the selection are example required BOG amount and shipyard construction capabilities.

2.3 Hull materials

Steel grade selection is based on design temperature, material thickness, and material class. Used steel grades with normal strength are A, B, D, and E grades. If steel with higher strength is needed, the options are AH, DH, EH, and FH grades. Steel grades' impact strength and fracture toughness capabilities are increasing from A grade to E grade. The difference between different steel grades is slightly different chemical composition and the used deoxidation practice. (Kendrick & Daley, 2011, p. 28; Räsänen, 2000, pp. 29-2-29-3)

The needed material thickness is based on strength stress calculations and ship weight optimization. Especially in the ice-going vessels, the mechanical stress burdens the ship hull at the bow and stern, depending on the ship type. The mechanical stress around the

LNG carrier hull in the cargo area is minor, but typically LNG carriers are quite long what exposes them midship sections to the different kinds of tensions. In general, the strengths of LNG carrier are determined by global wave bending loads. These loads govern the material thicknesses when the ice loads are not considered. In the areas which are facing ice loads the thicknesses have to determined based on the stress of ice load. Also, the temperature factor has to be noticed more carefully in this area while operating in the cold climate, and the cargo consists of cold LNG. The designer always has to compromise the material price and weight, sometimes steel grade with lower capacities might be good enough, but the needed thickness increases total ship weight compared to the usage of more advanced steel grade. When the ship's total weight increases, the required propulsion power increases, leading to higher fuel consumption during transportation.

Typically, the steel plate sections are shared to the smaller sections, and the steel grade selection is considered individually. An example of the steel grade selection for the inner hull in the USCG condition can be seen in Figure 4 (American Bureau of shipping, 2019, pp. 18-19). The inner hull needs a better steel grade because of colder temperature, as well the area above the water needs better steel grades than areas underwater.

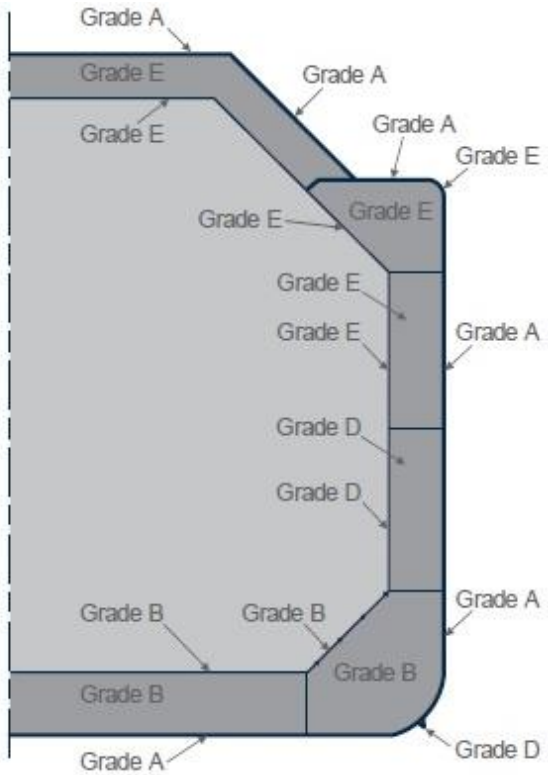

Figure 4 An example of the steel grade selection for the membrane tank in USDG conditions for inner hull and IMO condition for outer hull (American Bureau of shipping, 2019, p. 19)

2.4 Trunk deck, cofferdams and ballast tanks

The trunk deck's heating reflects the steel grade selection surrounding it and the design temperature of the trunk deck has to be considered during the thermal design. The space is large and requires a huge amount of energy when the space is kept warm in arctic conditions. Also, operational reliability has to be ensured. If the heating system fails, the piping between bow and stern becomes endangered. That can lead to problems for ship normal operations. Sometimes the nearest help can be far away, and the environment, cargo, and staff are becoming endangered.

Typically, trunk deck heating requires own individual heating units to ensure continuous heating in arctic conditions. The heat is typically implemented with a thermal oil system if the ship design temperature is extremely low. A water-glycol system or steam heating can also be considered. Heat is typically produced with boilers. The heat pump systems should be considered more in the future because cold sea or ambient air could be theoretically used as the heat source. A heat pump system requires electricity, but it can provide multiple times the energy back as heat (Grassi, 2018, p. 7). The advantages of heating oil systems are that the working pressure levels vary less than the water-glycol systems or heat pump systems.

The double hull structure is also used as the ballast tanks when it is required. For example, when the cargo tanks are not loaded, the ship is balanced by filling the ballast tanks. There is a possibility that the water on the ballast tank might freeze, especially in the arctic region. The situation is typically solved with heating coils. Circulating ballast water or air bubbling systems can also be an option for avoiding ballast water freezing. (Bagaev, et al., 2020, p. 2)

The cargo section is typically shared a couple of individual tanks. This enables support structure between starboard and portside and helps the instrumentation around the cargo tanks. The cargo has to be monitored continuously so the leakage will be noticed as soon as possible. Also, the cargo properties should be well known during the sail. In general, the cargo handling is also easier. The IGC code requires that the cofferdams must be heated, and the heating systems must have full redundancy. Each cofferdam has its own heating units, and the cofferdam space can be heated for example with heating coils. The

typical working fluid is a water-glycol mixture. Visualized view of the cargo tanks and cofferdams can be seen in Figure 5. (American Bureau of Shipping B, n.d., p. 16; GTT Training Ltd., 2015).

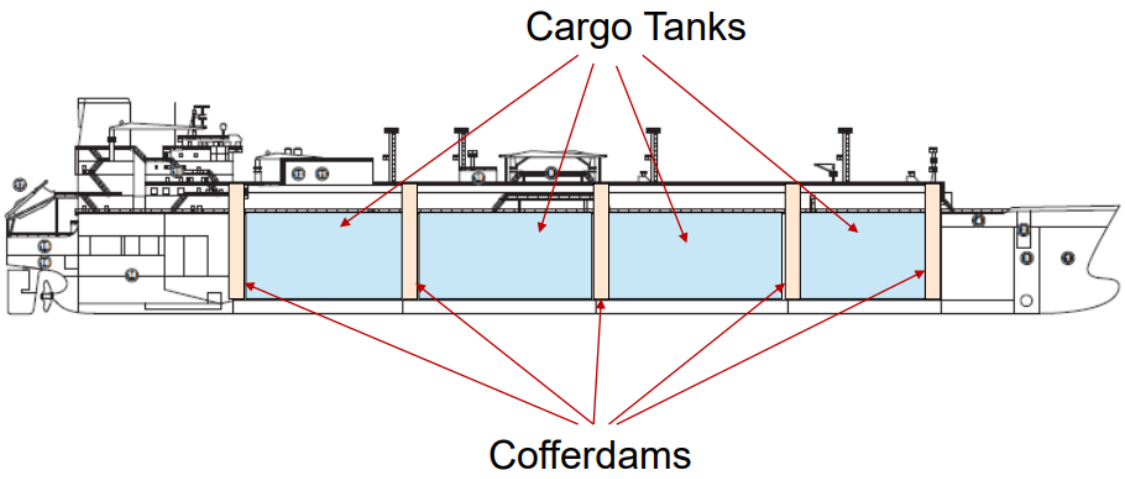

Figure 5 longitudinal view of LNG carrier. (GTT Training Ltd., 2015)

2.5 Tank damage scenario

Handmade assembly, thermal stress, and LNG sloshing expose insulations' first layer to the damage. If the damage happens, LNG flows inside the insulation box, as shown in Figure 6. After that, there is only secondary barrier layer left and its insulation between LNG and the inner hull. The local temperature of the inner hull starts decreasing and might reach critical temperature. The situation challenges the stability of the hull, and ship operation is becoming endangered. According to the IGC code, the ship must stand first barrier leakage for at least 15 days (IMO, 2014, p. 44).

The severity of damage is also depended on the used insulation system. Generally, if the damage happens, the damage is more serious for the Mark III system than NO96. In Mark III systems, the leakage can more likely go through to the second barrier also. There would be a high potential for hull damage if both barriers got damaged. (Choi, et al., 2012, p. 81)

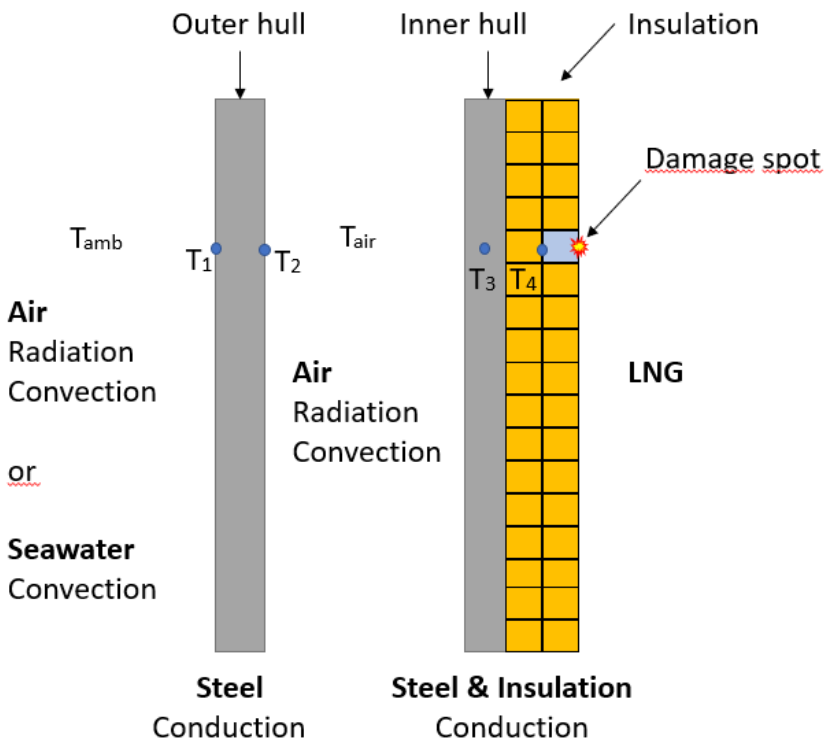

Figure 6 Visualized leakage situation

This situation should be investigated with transient simulations because the temperature development timely after the leakage is the most interesting aspect. The transient model requires a CFD model because the number of calculations increases significantly. As hard it is to predict the tank leakage situation, it can be imitated with simulation. The severity depends on the mass flow of the leakage and the formed crack size. Choi et al.(2012) investigated the leakage situation in their research paper. The study concluded that when the leakage crack is 5 mm or less and the mass flow is 0.01 g/s the thermal damage could be maintained as IMO's regulations are demanding. The study's model focused on the Mark III damage scenario where insulation primary and secondary barrier were damaged. But while reflecting this research paper's results to arctic region LNG container ship, it should be remembered that the critical crack size and the critical mass flow might be smaller if operated in the arctic region because the ambient temperatures are much lower than the temperature used in the Choi et al.(2012) research paper. Of course, this is depending on used steel grades and the clearance of the steel grade selection. (Choi, et al., 2012, pp. 82-89)

3 HEAT TRANSFER THEORY

Different physical phenomena in the LNG carrier midship section are presented in Figure 7. The total heat flux is positive from the environment to inside the tank because the environmental temperature is always warmer than LNG temperature. All the solid structures are transferring thermal energy by conducting. The ambient streams: water, and air, forms the convection effect to the outer hull. Basically, when the ship is moving, there can be spoken forced convection. Inside the hull structure, between the inner and outer hull, is forming free convection where driven force is temperature differences. (Qu, et al., 2019, pp. 106-107)

The radiation effect is the strongest above the ship's waterline but is affecting the whole structure. Inside the tank, ship movement is accomplishing convection in both gas and liquefied phase of gas. Total heat flux is positive to the inside tank and causes some of the LNG to boil. A part of it condensates on the cold surfaces back to the liquid phase. The sloshing, condensation, and boiling are not covered in this research paper.

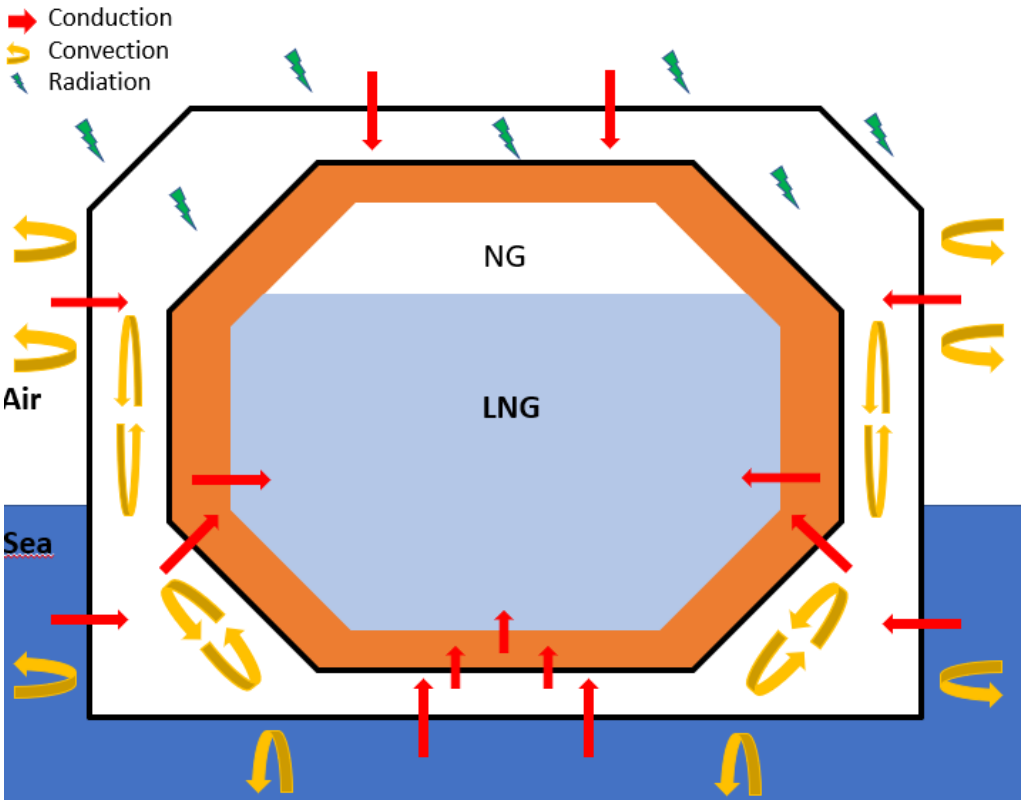

Figure 7. Midship section with different physical phenomena. (Qu, et al., 2019, p. 107)

Locally it is quite easy to build 1-Dimension heat transfer models. For example, to the shipboard, but using the 1-D model certainly gives a rough approximation of the real heat transfer situation. All heat transfer phenomena have 3-D nature in real life. When the number of dimensions is increasing, the calculation is becoming more complicated and heavier.

3.1 1-Dimension models

The horizontal heat balance from the shipboard can be seen in Figure 8. Building the calculation model for the 1-D situation Q_{total} the total heat flux can be defined to be equal with Q_1 and Q_2, where Q_1 is heat flux from outside of the ship to the compartment, and Q_2 is heat flux from the compartment to the LNG tank. The total heat flux is shown in Equation 3.1.

$$Q_{total} = Q_1 = Q_2 \tag{3.1}$$

The vertical heat transfer model on the cargo area top and bottom can be built with the same principle.

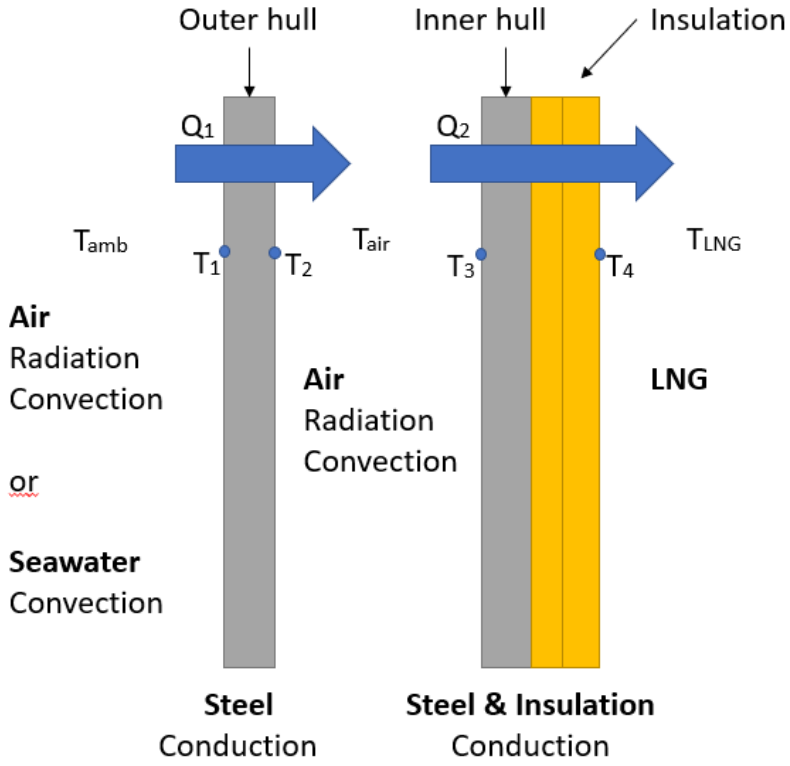

Figure 8. Horizontal heat transfer analysis model.

Heat transfer can be generally calculated as a function of overall heat transfer coefficient U, area of heat transfer A and temperature difference ΔT. Definition of heat transfer rate is shown in Equation 3.2. (Incropera, et al., 2007, p. 100)

$$Q = UA\Delta T \tag{3.2}$$

The overall heat transfer coefficient U consists of all factors of thermal resistance, convection, and conduction terms. Also, there should be paid attention to the contact resistances if absolute accuracy results are chased.

Conduction can be defined from material thickness t, thermal conductivity k, and temperature difference ΔT. The formula is known as Fourier's law. A heat flux of conduction shows in Equation 3.3. (Incropera, et al., 2007, pp. 4-5)

$$q''_{cond} = k\frac{\Delta T}{t} \tag{3.3}$$

The convective heat flux depends on the temperature difference between surface temperature T_s and environment temperature T_∞, and convection heat transfer coefficient h. The convective heat flux formula is shown in Equation 3.4. (Incropera, et al., 2007, p. 9)

$$q''_{conv} = h(T_\infty - T_s) \tag{3.4}$$

The convection heat transfer coefficient h depends on conditions in the boundary layer. The boundary layer conditions depend on fluid properties, surface geometry, and the nature of the fluid motion. The convection heat transfer coefficient can be defined with Nusselt number Nu, thermal conductivity k, and characteristic length L. The formula can be seen in Equation 3.5. (Incropera, et al., 2007, pp. 368-371)

$$h_{conv} = \frac{Nuk}{L} \tag{3.5}$$

The Nusselt number is a dimensionless number, and it tells the ratio between convective and conductive heat transfer on an interface. Empirical correlations are typically needed when figuring out the Nusselt number. Correlation selection is based on surface geometry and conditions. Typically correlations for the flat plate can be seen in Table 4.

Table 4 Correlations for the Nusselt number on a flat plane.

Correlation	Conditions	
$Nu = 0.332Re^{1/2}Pr^{1/3}$	Laminar, local,	T_f, $Pr \geq 0.6$
$Nu = 0.664Re^{1/2}Pr^{1/3}$	Laminar, average,	T_f, $Pr \geq 0.6$
$Nu = 0.0296Re^{4/5}Pr^{1/3}$	Turbulent, local,	T_f, $Re \leq 10^8$, $0.6 \leq Pr \leq 60$
$Nu = (0.037Re^{\frac{4}{5}} - 871)Pr^{1/3}$	Mixed, average,	T_f, $Re_c = 5 * 10^5$, $Re \leq 10^8$, $0.6 \leq Pr \leq 60$

The keys for choosing the suitable correlation are Reynolds number Re and Prandtl number Pr. The Prandtl number can be found from thermodynamic tables for most common fluids in atmospheric pressure when the temperature of the fluid is known. Also, it can be determined with specific heat c_p, dynamic viscosity μ, and thermal conductivity k. The equation can also be presented with thermal diffusivity α and kinematic viscosity ν. See Equation 3.6. (Incropera, et al., 2007, p. 376)

$$Pr = \frac{c_p \mu}{k} = \frac{\nu}{\alpha} \tag{3.6}$$

Reynolds number can be calculated as a function of fluid velocity u, fluid density ρ, characteristic length L, and dynamic viscosity μ. The Reynolds number can also be calculated with kinematic viscosity ν. The Reynolds number equation can be seen below in Equation 3.7. (White, 2011, pp. 27-28)

$$Re = \frac{uL\rho}{\mu} = \frac{uL}{\nu} \tag{3.7}$$

The transition from the laminar flow to the turbulent flow happens when the Reynolds number is about $5x10^5$. This critical value means that when the conditions are reached, most of the flow has turbulent nature and a laminar boundary layer becomes unstable. (White, 2011, p. 470)

Inside the compartment, between the inner and outer hull, the convection coefficient is a bit more complicated to determine because it is based on free convection. The free convection requires temperature differences which causes density differences between fluid particles. That causes movement on the fluid particles. The Rayleigh number must be defined in free convection calculation. The Rayleigh number describes the nature of the fluid when the density of the fluid is non-uniform. The Rayleigh number also clarifies is the natural convection forming or not. The theoretical value is considered to be 1708. If the natural convection is not forming, the heat is transferred by conduction between the fluid particles. Rayleigh number *Ra* defines as the sum of the Prandtl number *Pr* and the Grashof number *Gr*, as is shown in Equation 3.8. (Stephan, et al., 2010, p. 27)

$$Ra = GrPr \tag{3.8}$$

On the other hand, it can also be defined as the product of characteristic length L, gravity g, the thermal expansion coefficient β, kinematic viscosity v, the thermal diffusivity α, surface 1 temperature T_1, and surface 2 temperature T_2. This definition can be seen in Equation 3.9. (Stephan, et al., 2010, p. 27)

$$Ra = \frac{g\beta(T_1 - T_2)L^3}{v\alpha} \tag{3.9}$$

The thermal expansion for ideal gases can be calculated with Equation 3.10 seen below,

$$\beta = \frac{1}{T} \tag{3.10}$$

where temperature T can be approximated to be the average of T_1 and T_2, this average temperature should also be used to searching fluid properties. (Stephan, et al., 2010, p. 27)

When the Raleigh number is calculated, the empirical correlation for the Nusselt number calculation is needed. There can be used correlation a specific to the enclosures. If we look closer at the shipboard, there can be seen that because the environment temperature is warmer than LNG the outer hull is warmer than the inner hull, and the conditions for free convection are provided. Visualized principle schema of free convection in the enclosure can be seen in Figure 9.

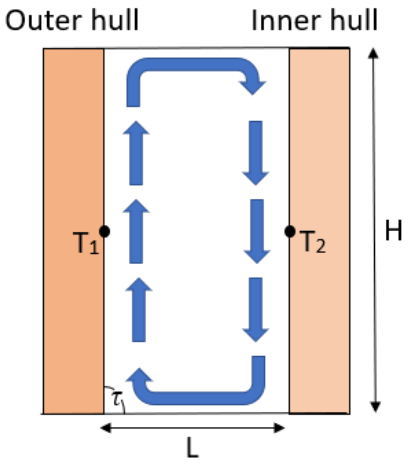

Figure 9 Enclosure and free convection. (Incropera, et al., 2007, pp. 588-589)

For the selection of the Nusselt number's correlation is affecting the tilt angle τ, Raleigh number *Ra*, Prandtl Number *Pr*, and aspect ratio *H/L*. The tilt angle describes the surface's angle from the horizontal plane position. The vertical enclosure with a heated surface, in this situation the outer hull, can be used correlation shown in Equation 3.11 when the aspect ratio is $2 \leq H/L \leq 10$, *Pr* is $\leq 10^{5,}$ and *Ra* $10^3 \leq$ Ra $\leq 10^{10}$. Horizontal planes are assumed to be adiabatic. When the tilt angle is different, or the situation does not fulfill the requirements different correlation has to be chosen.

$$Nu = 0.22\left(\frac{Pr}{0.2+Pr}Ra\right)^{0.28}\left(\frac{H}{L}\right)^{-\frac{1}{4}} \qquad 3.11$$

For example, in this investigation, the tilt angle is on the ship's bottom 0° and on the top of the tank 180°. The inner structure is always colder than the outer structure.

Another option is to use a simpler correlation for the free convection shown in Equation 3.12. The correlation can be generally used for the free convection situations on the wall plane. (Incropera, et al., 2007, p. 571)

$$Nu = \left(0.825 + \frac{0.387Ra^{\frac{1}{6}}}{\left(1+\left(\frac{0.492}{Pr}\right)^{\frac{9}{16}}\right)^{\frac{8}{27}}}\right)^2 \qquad 3.12$$

Radiation heat transfer coefficient may be presented, as shown in Equation 3.13, by emissivity ε, Stefan-Boltzmann-constant σ, and the temperature difference between surface temperature T_1 and environment temperature T_2. (Incropera, et al., 2007, p. 27)

$$h_r = \sigma\varepsilon(T_1^2 + T_2^2)(T_1 + T_2) \quad 3.13$$

Every material has its emissivity, and it is surface temperature depended. Stefan-Boltzmann-constant is 5,67x10^{-8} W/m^{2}K^4.

Let us look back at Figure 8. Based on the theory that has been gone through above, it is possible to calculate the total heat transfer from the environment to the compartment. And so on from the compartment to the tank. The overall heat transfer coefficient for U_1 and U_2 can be calculated as shown below in Equation 3.14 and 3.15.

$$\frac{1}{U_1} = \frac{1}{h_{c,\infty/OH} + h_{r,\infty/OH}} + \frac{t_{OH}}{k_{OH}} + \frac{1}{h_{c,OH/CO} + h_{r,OH/CO}} \quad 3.14$$

$$\frac{1}{U_2} = \frac{1}{h_{c,CO/IH} + h_{r,CO/IH}} + \frac{t_{IH}}{k_{IH}} + \frac{t_{INS}}{k_{INS}} \quad 3.15$$

And finally, Q may be calculated with Equation 3.2. After that, the total heat flux is determined, and how much heat is transferred from the environment to the tank is known. Exactly the total heat flux to the tank is not so relevant to know in this research. The main goal is to figure out the temperature distribution in the steel structure. The only initial temperatures for the design that are available are seawater temperature and air temperature. Material properties can be determined, and air and seawater velocities may be approximated. In other words, all the temperatures between the environment and LNG are unknown. Also, the total heat flux to the tank is unknown. This leads to the situation where the solution needs to be solved with the iterative process. The start of the calculation process needs a valid guess for the outer hull's outer surface temperature. Then the calculation can proceed forward. Theoretically, the calculations can be compared to the manufacturer's BOG gas values if the total heat flux from all sectors is

summed and transformed to the BOG amount. If the results are not facing the manufacturer values, the initial values of the calculation should be thought about again.

Building 1-D models might be a good option to see roughly view the temperature distribution from the tank surrounding structure, but as we know, using 1-D models does not give accurate results of the situation. For example, the conduction from structures below the waterline to structures above the waterline can be expected to be significant. In the 1-D model, these things are impossible to consider, and achieving accurate results is impossible. That is why 2-D models are typically required.

3.2 2-Dimension models

The 2-D conduction calculations are typically based on the finite difference method, where the entirety is shared to smaller pieces to the nodes. The nodes are created to be the same size, and after all the equation reduces a simpler format. The visualized schema can be seen in Figure 10. The number of nodes determines the accuracy of calculations. (White, 2011, pp. 579-582)

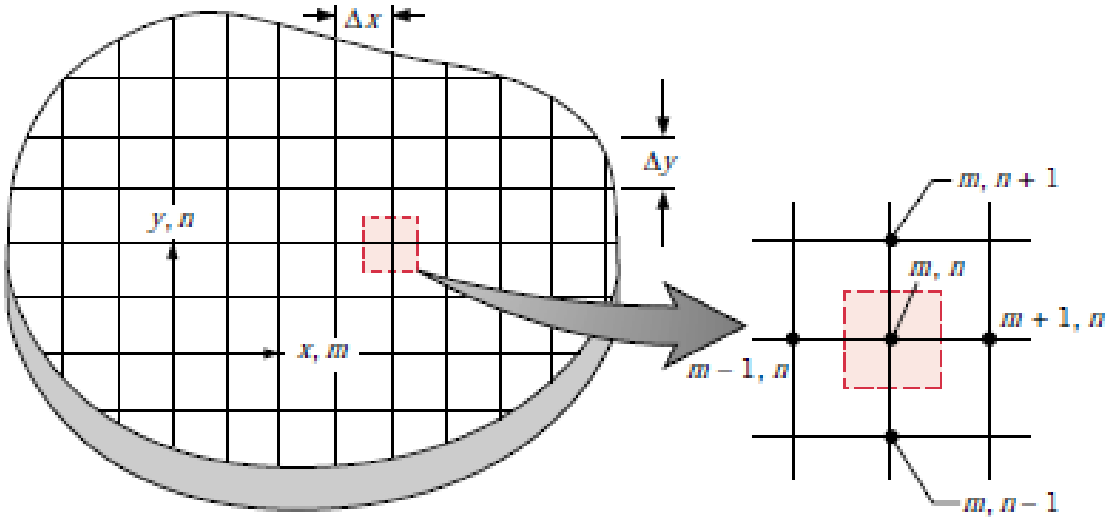

Figure 10 Principle schema of a nodal network (Incropera, et al., 2007, p. 213).

The temperature in the nodal point may be presented with the temperatures surround it if the thermal conductivity between nodes is assumed to be constant. If Δx=Δy, the form of

the heat equation depends only on temperatures surrounded nodal points. See Equation 3.16 below. (Incropera, et al., 2007, pp. 214-215)

$$T_{m,n+1} + T_{m,n-1} + T_{m+1,n} + T_{m-1,n} - 4T_{m,n} = 0 \quad (3.16)$$

It is also known that the energy balance method for steady-state conditions can be applied. It can be presented as below in Equation 3.17, where E_{in} is a rate of energy transfer into a control volume, and E_{g} is a rate of energy generation. (Incropera, et al., 2007, p. 215)

$$E_{in} + E_g = 0 \quad (3.17)$$

Energy to the node is influenced by conduction between the node and its adjoining nodes. Therefore equation 3.17 can be present as in Equation 3.18. (Incropera, et al., 2007, p. 216)

$$\sum_{i=1}^{4} q_{(i)\to(m,n)} + q(\Delta x \Delta y \cdot 1) = 0 \quad (3.18)$$

When thermal conductivity on the nodes is the same, and $\Delta x = \Delta y$ the equation can be reduced, as is shown below in equation 3.19. (Incropera, et al., 2007, p. 216)

$$T_{m,n+1} + T_{m,n-1} + T_{m+1,n} + T_{m-1,n} + \frac{q(\Delta x)^2}{k} - 4T_{m,n} = 0 \quad (3.19)$$

If there is no internal energy source in the node, the equation can be reduced, as shown in Equation 3.16.

When there is also convection affecting the node, for example, the outer hull interface case, the nodal finite-difference equation gets its form as shown in Equation 3.20. (Incropera, et al., 2007, p. 218)

$$\left(2T_{m-1,n} + T_{m,n+1} + T_{m,n-1}\right) + \frac{2h\Delta x}{k} T_\infty - 2\left(\frac{h\Delta x}{k} + 2\right) T_{m,n} = 0 \quad (3.20)$$

If the radiation and convection want to be taken into account, the equation with uniform heat flux can be used below in Equation 3.21. (Incropera, et al., 2007, p. 218)

$$\left(2T_{m-1,n} + T_{m,n+1} + T_{m,n-1}\right) + \frac{2q''\Delta x}{k} - 4T_{m,n} = 0 \qquad 3.21$$

Visualized balance figures for equations 3.20 and 3.21 can be seen in Figure 11.

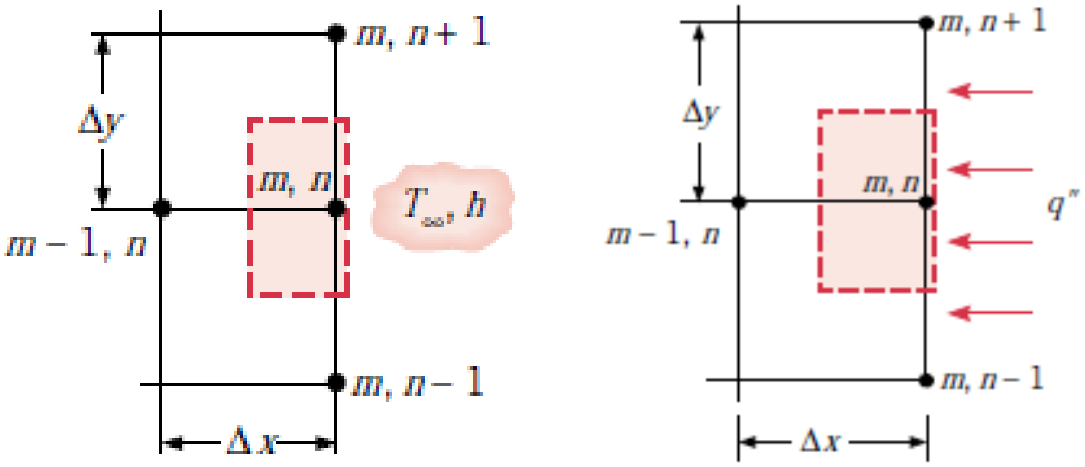

Figure 11 Visualized balance sheet of 2-D heat transfer cases (Incropera, et al., 2007, p. 218).

If the nodes are unstructured, the equations are not reducing to a simple form. Also, when there are interfaces between the inner hull and insulation, the equations are not reducing as nice, because the conductivities of materials are different. Otherwise, if the nodes are the same size and conductivity is not changing, the formed equations can be solved by putting them in a matrix format, and then they are theoretically quite efficient to solve (Incropera, et al., 2007, pp. 222-223).

As we can see, the competence of required calculations increases significantly when the 2-D solution wants to be achieved. In practice, in larger 2-D models, as in this case, it is not efficient to calculate manually. But with CFD software calculating 2-D models is quite efficient and certainly informatic. The one problem that comes to the 2-D modeling in CFD is the wind and sea flow direction. The designer cannot set z-direction flows that are relevant while considering the ship operation in real life.

3.3 3-Dimension models

3-D models are based on the same theory as 2-D models, but the node also has adjoining nodes on the z-direction. As simplified, the size and the number of equations increase. Practically this leads to a situation where manual calculations are rejected. It is possible to use 3-D models in CFD software, but it requires more calculation power which means it takes more time to run simulations than in 2-D. The 3-D CFD models give the most realistic results from the whole entity. For example, the flow directions can be set as they are in natural phenomena. But on the other hand, practical 3-D models are the most challenging to build. The used time will always not cover the achieved results if they are compared to 2-D applications.

4 A BRIEF FUNDAMENTALS OF CFD

The CFD theory has grown its roots during the last centuries. The biggest step in the modern CFD theory was taken between the ’60s and ’80s (Jameson, 2012). Firsts commercial software were published in the early ’80s. After that, they were used only inside the small circuits for a long time. Nowadays, when commercial software has developed to more user-friendly and computers’ computational power has increased significantly during the last decades, its usage has become more and more to the designers' daily working tool (Anderson Jr., et al., 2009, pp. 6-8).

CFD procedure can be divided into three individual sections: preprocessor, solver, and postprocessor (Tu, et al., 2018, pp. 33-34). Visualized figure from the CFD procedure and its main aspects can be seen in Figure 12.

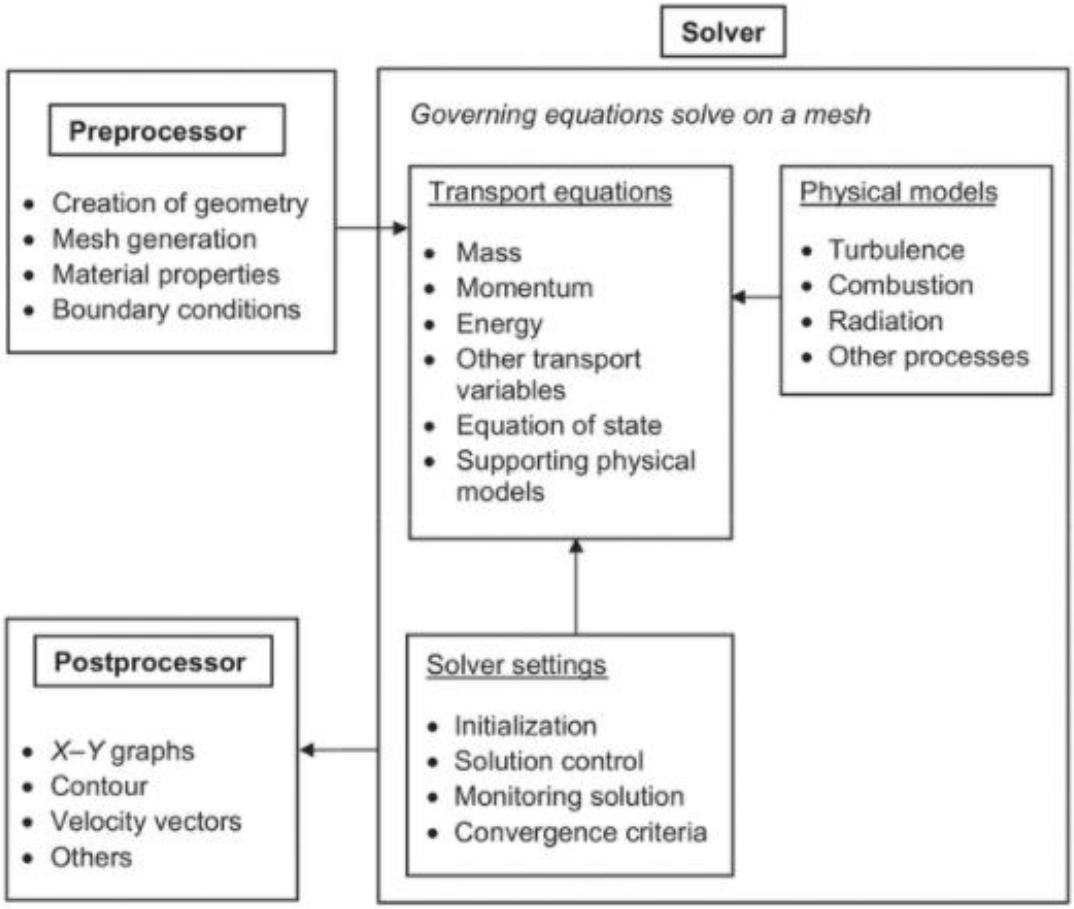

Figure 12 CFD-based solution procedure main aspects (Tu, et al., 2018, p. 35).

4.1 Preprocessing

Before simulation can be started, the model geometry has to build. Important things that should be considered for geometry drawing are that the geometry should be simple enough but also accurate enough to describe the actual geometry. Nowadays, there is plenty of commercial software options for geometry drawing.

After geometry is created, the next step is to do mesh. The mesh is the form of the nodal network, which was described in Chapter 3.2. Mesh structure can be divided into structured meshes and unstructured meshes (Tu, et al., 2018, pp. 127-136). Typically structured mesh should be preferred if possible because it is more efficient to calculate, and discretization has better accuracy. If the geometry has a more complicated shape, then the geometry isn`t fitting structured mesh, and it has to have meshed with unstructured mesh shapes. A good thumb of rule is to use structured mesh in the geometry where it is possible and other locations to use unstructured mesh. Common cell shapes for the 2-D models are tringles and quadrilateral, and tetrahedron, pyramid, and hexahedron for the 3-D models.

The number of cells describes mesh quality. Correctly built mesh has denser mesh near boundary layers (Tu, et al., 2018, p. 141). In the other areas which have no boundary layers and flow has assumed to have laminar nature is no need to use dense mesh. This increases the efficiency of calculation. For the determination of mesh, density can be used dimensionless wall distance $y+$. Also, cells' aspect ratio is an excellent parameter to be monitored while ensuring the mesh quality (Anderson Jr., et al., 2009, p. 313).

Material properties and boundary conditions must be determined before the movement to the next phase can be done. Material properties can be set manually or searched from the CFD program material library.

Preprocessing has significant effects on the final results. For that reason, especially the mesh building, boundary conditions, and made assumptions for the whole model should be considered carefully.

4.2 Solving

CFD software conceals numerical theory inside the program code. While using the program, there is no need to write numerical theory for the calculations. The results understanding and how the calculation process is done inside the code, it is required. This requires at least the basic knowledge of the numerical methods (Tu, et al., 2018, p. 46). Transport equations are solving the interaction between the nodes. At first, the physical models have to be determined, and that practically determines what is solved and taken into account during the simulations. And finally, before the start of the simulation, the solver settings must be done. Most important is to initialize the model and decided the number of iterations and convergence criteria. Typically the developments of the residuals are monitored during the simulation. If it seems that the residuals will not convergence nicely, it should be considered to shut down the process. If it seems that the convergence criteria on the residuals are possibly achieved, the simulation should run till to the end. (Tu, et al., 2018, pp. 46-48).

The default residuals in FLUENT are not providing the only way to successful results. In complex problems, especially the continuity might stay certainly high. It is not always mean that the model is not converging. Continuity is dimensionless, so it will not always achieve as low a value as other default residual. Also, the FLUENT residuals are scaled values, so the values are not absolute values in the monitor (ANSYS, 2013, pp. 1477-1479). For double-checking the convergence, it is recommended to monitor some extra variables, such as temperature or pressure during the iterations.

4.2.1 Governing equations

CFD modeling is based on the governing equations which are representing the conversation laws of physics. The main governing equations are mass, momentum, and energy conversation equations. The equations are describing how fluid pressure, temperature, velocity, and density are related. The Navier-Stokes equations consist of time-dependent equation for each of these. The Navier-stokes equations' basic forms are acceptable to use when the fluid flow is laminar. But while computing turbulence applications, the equations should be modified to make the calculation results reasonable in a reasonable time. Practically RANS (Reynolds-averaged Navier-Stokes) equations are

solved for the turbulent flows, and these govern the mean flow in the turbulence model. (Anderson Jr., et al., 2009, pp. 321-323)

There is a different type of solvers available for the solving process. A pressure-based SIMPLE-algorithm (Semi-Implicit Method for Pressure Linked Equations) is used during this study. (Tu, et al., 2018, pp. 65-113)

4.3 Post-processing

After the simulation is done, the results should be post-processed. For example, different kinds of x-y graphs, contours, and velocity fields can be drawn (Tu, et al., 2018, pp. 52-61). Those are the ways how to visualize the results and dick out the wanted matters. In this phase, there are no possibilities to affect anymore to the results.

5 CALCULATION MODELS

This chapter handles how the hull steel temperatures can be determined with handmade manual calculations and with CFD software. At first, the handmade calculation is executed, and the CFD simulation's simplifications are based on the findings from manual calculations. The manual model has executed with the 1-D format, and the CFD models were executed in 2-D format.

The geometry of the CFD model was created by using Ansys Space Claim, the mesh was created with Ansys Mesh, and the simulations were executed with Ansys Fluent. Used Ansys license of this study was the Ansys student license. Student license has some limitations. For example, the maxim number of nodes for the model is 512 000 nodes. There was decided to use ANSYS's FLUENT because access to the license is easy, and it is widely used in the research field and student communities.

5.1 1-D manual model

The 1-D model calculation gives a rough result of the temperature distribution in the ship hull structure, but it is a relevant way to investigate which phenomena effects to the entirety. Then the simplifications and boundary settings can be determined to the more complicated 2-D and 3-D calculations.

With a 1-D model, the solution can be based on equivalent thermal circuits for shipboard. The equivalent thermal circuit means that the energy between the layer is not disappearing anywhere. In other words, heat is transferring only in 1-D. The same amount of energy is going through in every section. That is a good way to make calculations easy to execute. The heat transfer rate can be determined as shown in equation 5.1. Principle schema for the calculation can be seen in Figure 13. (American Bureau of shipping, 2019, p. 10)

$$\frac{Q}{A} = \frac{T_{amb} - T_1}{\frac{1}{h_{tot}}} = \frac{T_1 - T_2}{\frac{L_{steel}}{k_{steel}}} = \frac{T_2 - T_{air}}{\frac{1}{h_{tot,2}}} = \frac{T_{air} - T_3}{\frac{1}{h_{tot,3}}} = \frac{T_3 - T_4}{\frac{L_{steel}}{k_{steel}}} = \frac{T_4 - T_{LNG}}{\frac{L_{perlite}}{k_{perlite}}} \quad (5.1)$$

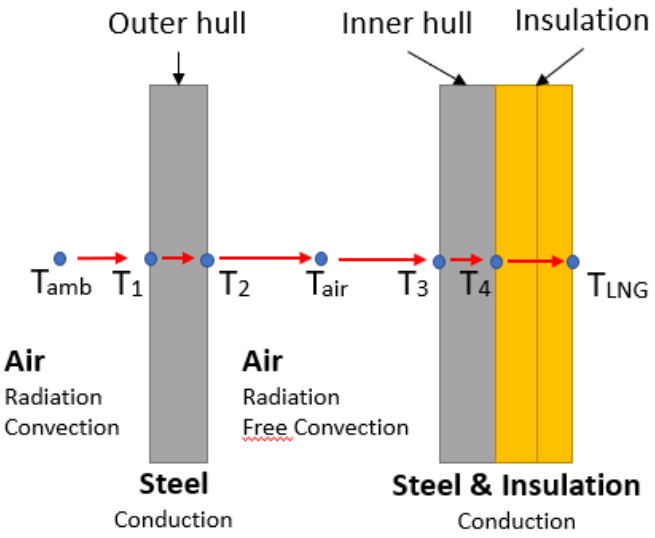

Figure 13 Principal schema for the manual calculation.

Total convection heat transfer coefficients can be determined by summing the relevant factors as is shown in Equation 5.2 to the outer hull's outer surface, where convection and radiation have to be taken into account. This is based on the basic theory behind the overall heat transfer coefficient U.

$$h_{tot} = h_r + h_{conv} \tag{5.2}$$

The main boundaries and material properties which is used in the calculation are listed below.

- The ambient air temperature is -50°C, and velocity is 5 m/s.
- Seawater temperature is 0°C, and velocity is 5 m/s.
- Steel plate's thickness is 20mm, and conductivity is 20 W/m·K. Steel emissivity was set to be 0.2.
- CCS is simplified with 530mm thick expanded perlite. Perlite conductivity is 0.02 W/m·K.
- The temperature in the first barrier is assumed to be as LNG temperature -163°C.

There were build three different types of calculation tools in MS Excel on both sides of the waterline. The real geometry is not as simple as was drawn in Figure 13. For example, the hull structure consists of different kinds of support structures, which could be treated as fins from the thermal design perspective. For example, bolts and beams, but the effect of fins was not taken into account. In case 1, the insulation structure was simple one thick

perlite layer, and radiation was not taken into account. In case 2, the insulation structure was still kept as in case 1, but the radiation effect was taken into account. In case 3, the insulation structure was defined as the actual insulation structure. Contact resistances were approximated, and all the actual layers of insulation structure were taken in the calculations. The radiation effect was included in the third case. Table 5 and Table 6 show how markable the radiation effect in this case is and if the insulation structure is as well simplified to be as a one layer how it distorts the temperatures.

Table 5 Temperatures from ambient air to inner hull.

Case	T_{amb} [C°]	T_1 [C°]	T_2 [C°]	T_{air} [C°]	T_3 [C°]	T_4 [C°]	T_{LNG} [°C]
1	-50	-50,51	-50,51	-52,40	-54,29	-54,29	-163
2	-50	-50,48	-50,48	-52,37	-54,26	-54,26	-163
3	-50	-50,47	-50,48	-52,35	-54,22	-54,22	-163

Table 6 Temperatures from sea water to inner hull.

Case	T_{amb} [C°]	T_1 [C°]	T_2 [C°]	T_{air} [C°]	T_3 [C°]	T_4 [C°]	T_{LNG} [°C]
1	0	-0,55	-0,56	-3,26	-5,95	-5,96	-163
2	0	-0,51	-0,52	-3,21	-5,90	-5,90	-163
3	0	-0,51	-0,51	-3,18	-5,84	-5,85	-163

The radiation effect is almost negligible. The specific insulation structure versus one simplified thick layer did not make a big difference. The significance of the effect can be assessed as moderate, but from the steel grade selection point of view, the effect is minor.

In the third model, the effect of contact resistances and exactly layers of insulation structure effect were investigated. The challenge of determining the contact resistances is that the contact resistance is always dependent on contact pressure, and it also depends on how the layers are connected (Incropera, et al., 2007, pp. 102-103). The contact between two layers is never perfect and always contains some air gaps between layers. If the contact is smoother, the contact resistance is minor. And if the contact is rougher, the contact resistance is more significant. Practically these things are hard to determine without empirical knowledge. These calculations were executed based on principles of physics and available data from the research field (Babu, 2015, p. 16).

The stream velocities effect on the thermal design was investigated by increasing the seawater and ambient airflow velocities. It can be stated that the velocities had minor effects on the steel structure temperatures. When velocities were increased, it was

favorable the steel structure temperatures. The ambient streams' internal energy is then more available, and more heat flows through to the structure. It has to be remembered that even though the streams' effects are negligible from the steel grade design point of view, it might be more markable example cofferdam heating point of view.

5.1.1 Validation of the calculations

The calculated temperatures for the hull steel structure were validated by calculating the amount of BOG. The aim was to look at whether the calculated BOG corresponds to the manufacturer values at any level. It was assumed that all the heat flux that flows inside the tank evaporates LNG. The heat flow from the tank gables was not considered. Also, the trunk deck heating, radiation, contact resistances, support structures (thermal fins) were not taken into account.

At first, the BOG was calculated with the same boundary conditions values as the temperatures earlier. The calculated BOG value was 0,02 %. After that, the boundary conditions were changed to IGC code warm conditions, so the value is easier to compare to the manufacturer value. The calculated BOG value was 0,04 %. It can be stated that with these simplifications, the calculated values are reasonable. The calculated values are smaller than the manufacturer's values, and the simplifications mainly cause this. The manufacturer's BOG values are from 0,15% to 0,07%, and they were presented more precisely in chapter 2.2.1. For example, the heat flux from the gables can be assumed to be significant. In the colder conditions, the BOG value is smaller as it should be. And even the calculated value is not facing exactly the manufacturer's values, their scale is good. Without knowing the exact arrangement of the tanks, how many individual tanks are on the ship, what are the temperatures in the cofferdam between the tanks, what are the service temperatures in the spaces next to the tanks in stern and bow, etcetera, it is impossible to calculate a more accurate value for the BOG. The calculated BOG values follow the general scale for the BOG values, and they are ensuring that the manual calculation is properly solved.

5.1.2 Boundaries for the CFD models

As was expected, the effect of radiation is almost negligible from steel structures' temperature point of view. The effects were seen in the temperatures' second decimal. The effects of contact resistances in the CCS structure were calculated to be minor as well. When the contact resistances were taken into account, it was seen in the temperatures' first decimal. The sum of the effects of radiation and contact resistances has a minor effect on the steel structure temperatures. For that reason, modeling of them can be ignored. This makes the design work much more efficient, especially in multidimensional CFD models.

5.2 CFD model

At first, the CFD modeling process was started by creating geometry. The used dimensions were got from Aker Arctic internal materials. The built model has a typical dimensioning for Arctic region LNG carriers. The first aim was to build a CFD model where ambient air and seawater flows are taken into account in the model. During the modeling process, it was noticed that the models with seawater and ambient airflow are not converging during the simulations. The main reason for that was the model's complexity and limited node amount. For that reason, the models had to be simplified. The working models consist of steel structure, air compartment inside the steel structure, cofferdam space, and CCS insulation. The models were executed in 2-D format.

5.2.1 Geometry

In the drawing of the model carrier's midship-section, there were used typical dimension of the artic LNG carrier around 150 000 m^3 capacity. The outlines of the ship were drawn first. After that, the steel thicknesses in different sections of the ship were taken into account. In the end, the insulations of the cofferdam and CCS were drawn. The geometry can be seen in Figure 14.

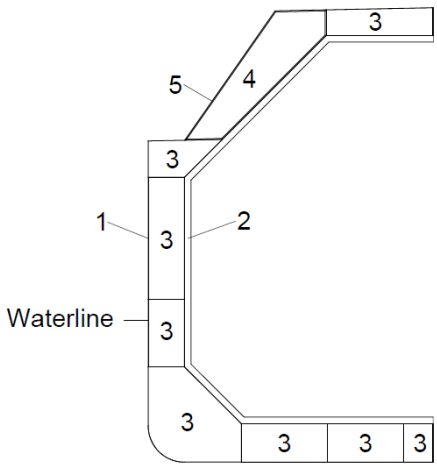

The numbers are clarifying model as following way:

1. Steel structure
2. CCS system insulation layer
3. Compartments, the air closets between the steel structure
4. Heated trunk deck
5. Trunk deck insulation

Figure 14 The basic geometry of the CFD model.

As we can see, the model geometry is a simplified version of the real geometry of the midship section and does not include supporting structures or deck equipment. The CCS structure is simplified to be as one layer. As was investigated in the manual calculation, if the thickness in the insulation layer is the same as the total thickness of all layers in real geometry, it is acceptable to simplify the geometry. This makes the meshing process a lot lighter. Especially the thin barriers on the real geometry would require calculation power and challenge the meshing settings.

The steel plates have a thickness between 15-25 mm, depending on location. The insulation layer is 530 mm thick, and the trunk deck insulation is 80 mm thick. The model is about 20 m wide and 35 m height. The ship waterline can also be seen in Figure 14.

The filling limit of the cargo tanks is 98% of the tank capacity (IMO, 2014, p. 137). It was assumed that the top barrier of the tank had approximated the same surface temperature as the other surfaces in the tank. During the worst-case scenario, this is an acceptable simplification.

The tank insulation is drawn as one solid body because the contact resistances' effect on heat transfer phenomena is minor. This was stated previously in this study. As well as the contact resistance is not easy to specify in the Ansys without previous knowledge and the specific info of the used materials (ANSYS, 2013, pp. 317-318).

5.2.2 **Mesh**

The mesh building has a major role in successful CFD modeling. At first, there were considered how dense mesh should be built in the air – steel interfaces inside the compartment. Typically first layer thickness should be around 10^{-3} to 10^{-5} m, depending on the surface roughness, fluid properties, and flow velocity. But in this model, the fluid flow has slow velocities, and extremely thin mesh is not necessarily required. In some cases, too thin mesh might cause problems, such as numerical errors (Boz, et al., 2014, pp. 13-15). Typically the best solution is achieved with an executed mesh-sensitive analysis.

If the boundary layer's thickness is set to be thin, the side effect might be the increased aspect ratio. On the other hand, the cell size can be increased in the areas which are not next to the walls. But this problem may challenge the mesh quality and affect the results or residuals convergence. (ANSYS, 2013, p. 132)

In this research, the solid structures aren't facing any mechanical analysis, so there is no need to fine mesh in solid parts. When the part has achieved acceptable quality for the nodes from the converging point of view, it is good enough because more nodes require more computing power. If the temperature distribution advancement wants to be monitored the more nodes are needed. But in this kind of application, solid parts are generally homogenous with a simple structure, and the temperature changes linearly. There is no interests in monitoring the temperature development, for example during the insulation layer.

The geometry was created with Ansys Mesh. In the program, a sizing tool was used to refine the meshes. With refining tools, the space next to walls meshed denser. Also, necessary sections were named for the boundary conditions set to the next phase.

There were build three types of mesh: mesh A, B, and C. The mesh A is finest, the mesh B is medium-fine, the mesh C coarsest. The mesh A is quite close to the student license limit. The main aim for doing different meshes was to investigate the mesh usability and how it affects forming free convection and the steel structure temperatures. The simulation convergence time and quality were also monitored.

In the mesh A and mesh B were used high smoothing. The C mesh was done by medium smoothing. The smoothing describes the transection from the denser mesh to the coarser mesh, and typically with higher smoothing the convergence is more probably achieved. The first layer thickness and number of elements and nodes can be seen in Table 7. The mesh resolution in the steel structure, trunk deck's and CCS's system insulation were kept constant. Only the fluid calculation boundary was varied.

Table 7 Properties of the meshes.

Mesh	Nodes	Elements	First layer element size in the free convection layers [m]
A	485 960	460 859	$7.0 \cdot 10^{-3}$
B	257 631	232 710	$7.0 \cdot 10^{-3}$
C	153 491	132 464	$1.4 \cdot 10^{-2}$

The slices of the meshes can be seen in Figure 15, Figure 16, and Figure 17. The green and brown colors are air computational domains, the grey-green is the tank insulation and the steel structure goes on the left edge, between fluid domains, and between insulation and fluid domains. The nodes in steel structure are hard to see in pictures because it is so thin when compared the total model size.

As we can see the mesh A is much denser than B and C mesh. Its structure is nearby structured. On the other hand, the mesh B and C seem to have about the same node size in fluid domains, except the mesh B has denser mesh next to the steel structure.

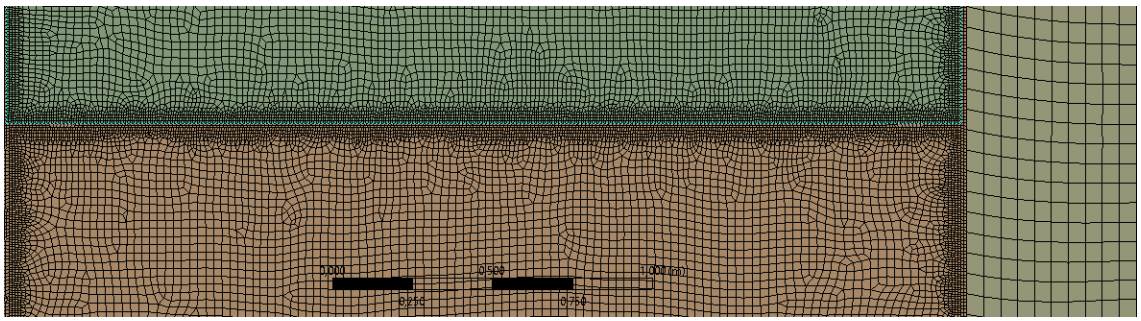

Figure 15 Mesh A.

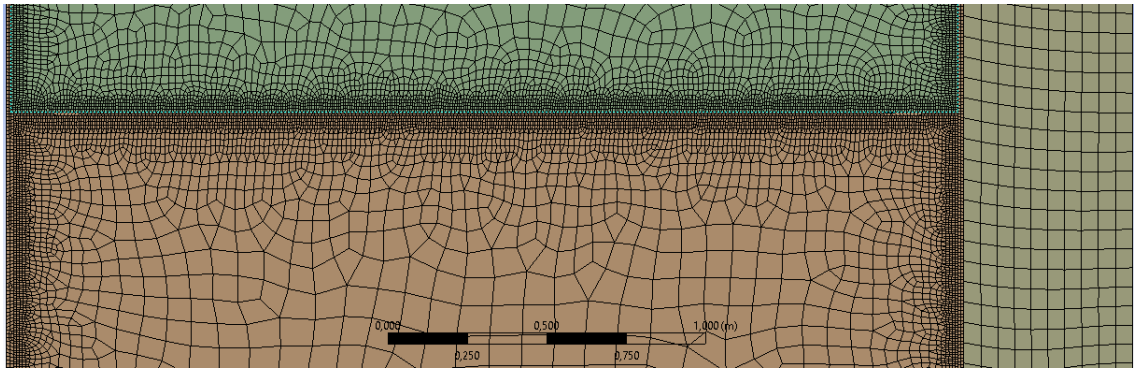

Figure 16 Mesh B.

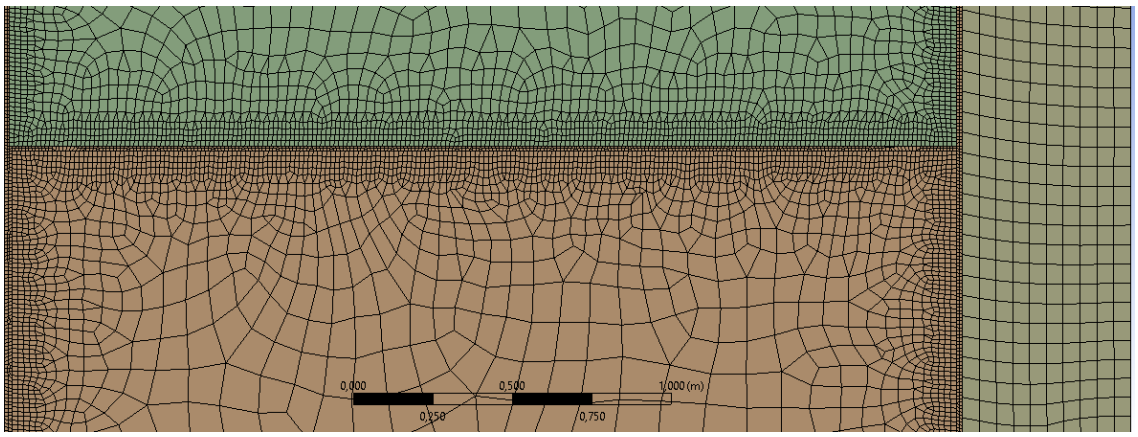

Figure 17 Mesh C.

5.3 Simulations

The simulation was done by using the SST k-omega model with pressure-based solver SIMPLE. SST k-omega is blend of k-ω and k-ε models (ANSYS, 2013, pp. 698-690). It is widely used in the research field and industry (Simscale, 2021). The viscous heating was set on, and the buoyancy effects were set to full mode. The gravity was set to be -9.81 m/s in the y-direction. In free convection application, it is absolutely important that the gravity is on in the models and the buoyancy effects are considered during the simulation because otherwise, the free convection is not forming. Solution controls, the under-relaxation factors were used Fluent's default values.

5.3.1 **Boundary conditions & material properties**

The cofferdam's walls were set to be 5 °C, and the tank insulation inner wall to be -163 °C. The outer hull's outer wall was set to be in above water -51 °C & underwater -1 °C based on manual calculation. These boundary conditions are realistic to use when the focus is on the worst-case scenario.

The used insulation material for the tank insulation was defined to be expanded perlite. Expanded perlite and polyurethane foam have approximately the same thermal properties as shown in Figure 18, so there was no significant difference in which one is used during the simulation (Choi, et al., 2012, pp. 77-78).

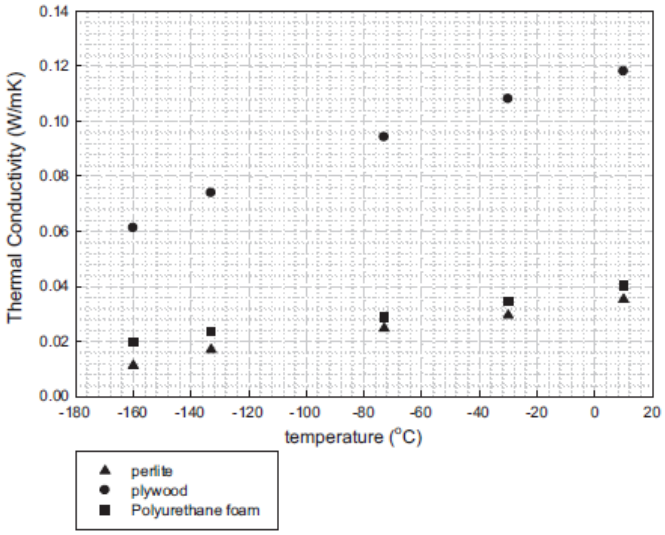

Figure 18 Thermal conductivity of the plywood, perlite, and PUF. (Choi, et al., 2012, p. 78)

Material properties can be defined to be constant values in the Fluent. Another option is to define some of the properties with a piecewise-linear profile tool. When the simulation's main aim is to do thermal analysis, using the piecewise-linear profile tool to define the materials' properties is a valid option because conductivity and other properties are always temperature-dependent. The piecewise-linear tool usage is highlighted, especially when the simulation consists of large-scale temperature differences. In this research, constant values or usage of piecewise-linear profile for material properties will not make a big difference because the temperature differences are moderate, only a couple of tens except the tank insulation layer.

In this investigation was decided to use constant values for air, steel, and rock wool. For the tank insulation there decided to use a piecewise-linear profile. Listed material properties can be seen in Table 8. Air density was set by using the Boussinesq approximation. Although the Boussinesq is a minor part of the whole simulation process, it is crucial to use it, so that reasonable results are achieved (ANSYS, 2013, p. 769). Otherwise, the natural convection is becoming distorted. The Boussinesq approximation was used because the ANSYS user’s guide is recommending to use it while simulating

natural convection applications. Air properties could also be set in other ways, for example using the ideal-gas setting option.

Table 8 Materials' properties. (Vepsäläinen, et al., 2012, pp. 193-210; Choi, et al., 2012, p. 78)

Section		Hull	Tank Insulation	Cofferdam Insulation
Material		Steel	Perlite	Rock wool
Density	[kg/m^3]	8000	50	100
Specific heat	[J/kgK]	500	387	1000
Conductivity	[W/mK]	20	See Figure 18	0.035
Viscosity	[kg/ms]			

5.3.2 **Residuals convergences, mesh sensitive analysis & computational time**

From the temperature distribution of point of view, these three types of meshes have no big differences in the temperature distribution. The final temperature balances of each mesh are comparable. In Figure 19 and Figure 20 can be seen mesh C residuals. Mesh A and B have approximately the same iteration profile, but the residuals took longer to achieve convergence.

Mesh C has the coarsest mesh, so it converges fastest. Mesh C and B converge certainly fast because they have fewer nodes than Mesh A. Mesh A takes the longest time per iteration loop and the highest number of iterations to achieve convergence. The mesh A required about 65 000 iterations loops for achieving the total convergence. For double-checking the meshes' convergence, the velocity in one compartment was monitored during the iterations. That was a good way to inspect that the convergences are achieved because the residuals oscillate at the final convergence stage.

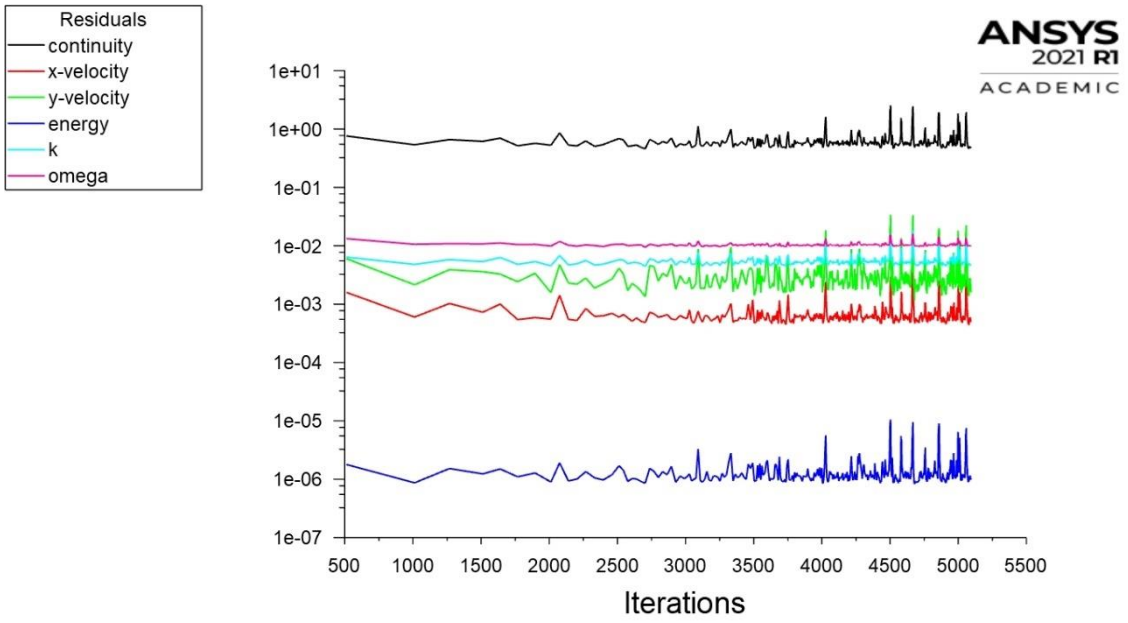

Figure 19 Mesh C's residuals.

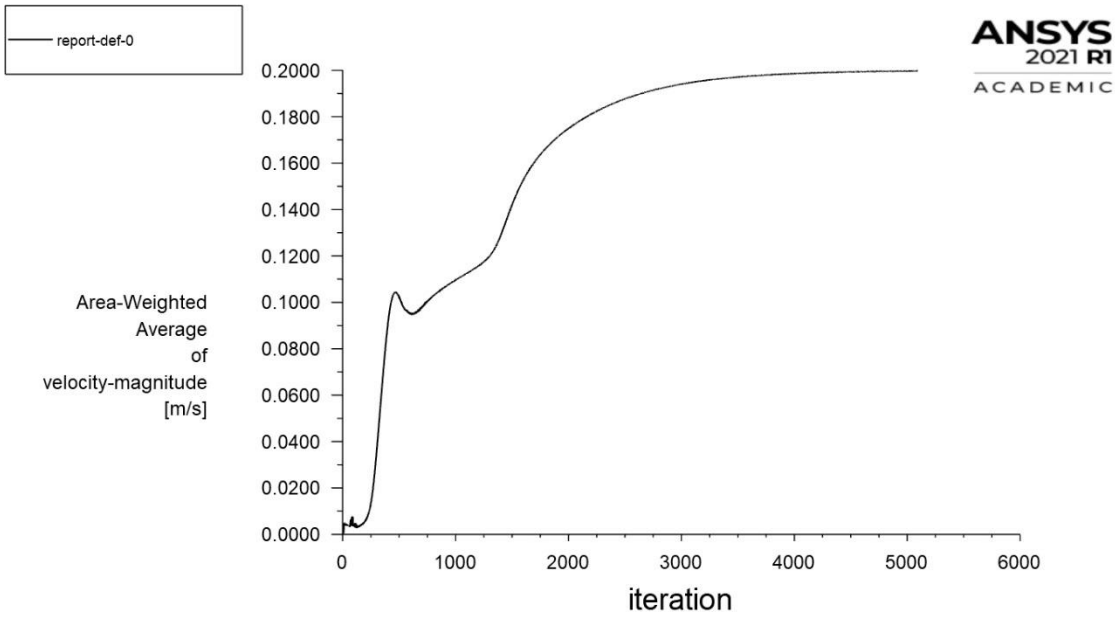

Figure 20 Mesh C's natural convection velocity development in the investigated compartment.

5.3.3 **Temperature distributions**

In general, the hull temperature follows given boundary values. The general view of the temperature distribution of the model can be seen in Figure 21. As we can see, the coldest temperatures are forming next to the LNG and the insulation structure. Temperatures are increasing linearly during the insulation layer. The insulation capability is affecting the

inner hull temperature. On the other side, the sea temperature and air temperature are mainly affecting the outer hull temperature. The air temperature in compartments is settling between the inner and outer hull temperature. Temperature contours for all simulations can be found in Appendix III.

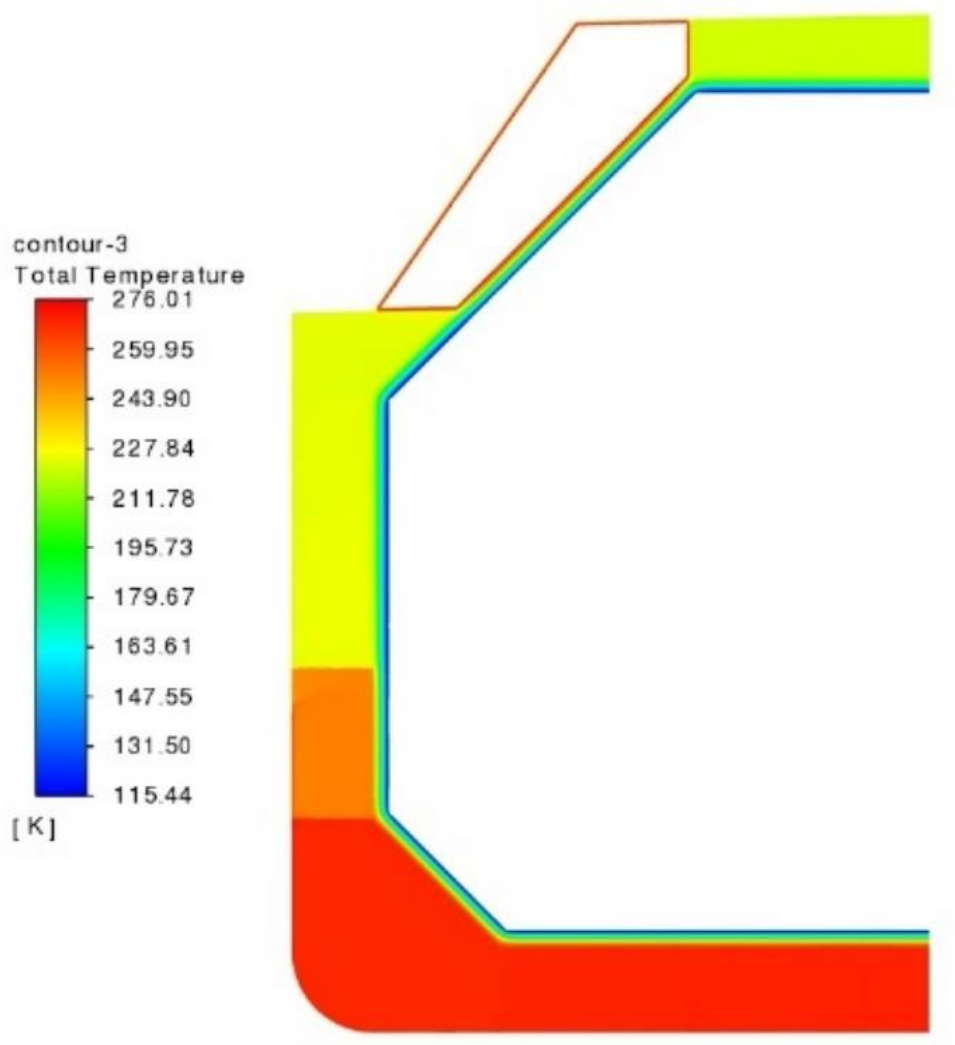

Figure 21 Temperature distribution of mesh C.

The post-processing process focused on the inner hull's steel because the temperatures in the outer hull follow strongly ambient air and seawater temperatures, so it is not relevant to focus on them. Also, the model and its boundaries are not deserving of the outer hull temperatures investigation. Therefore, all the three different models and their inner hull average temperatures were post-processed. The temperatures in the local points of the inner hull, as are pointed in Figure 22, were listed in Table 9. It is easier to follow listed values than post-process pictures because the model is large, and the hull temperatures are challenging to visualize.

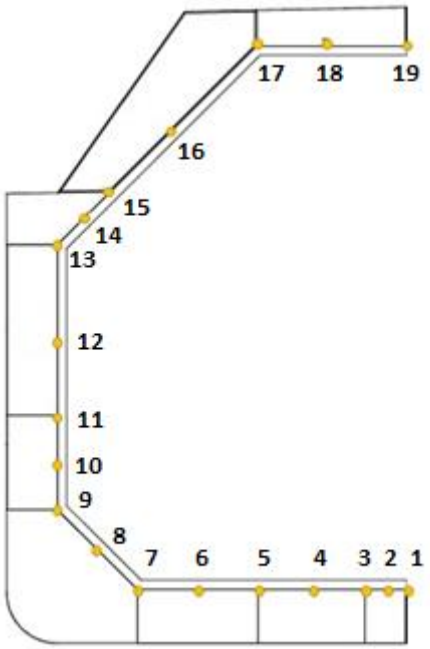

Figure 22 The post processed local points of inner hull.

Table 9 Inner hull's temperatures from the bottom to the top.

Point	Mesh A [°C]	Mesh B [°C]	Mes C [°C]
1	-6,0	-5,5	-6,0
2	-6,0	-5,5	-6,0
3	-6,0	-5,5	-4,4
4	-6,0	-6,4	-6,0
5	-6,0	-6,4	-6,0
6	-6,0	-6,4	-6,0
7	-6,0	-6,4	-6,0
8	-7,6	-7,2	-7,6
9	-14,0	-12,8	-14,0
10	-22,0	-22,4	-23,6
11	-33,3	-34,4	-34,9
12	-50,9	-49,6	-49,3
13	-49,3	-50,4	-49,1
14	-49,3	-52,8	-49,3
15	-33,3	-38,0	-36,5
16	-7,6	-8,0	-9,2
17	-42,9	-42,4	-42,9
18	-54,1	-53,6	-52,5
19	-52,5	-52,0	-52,5

As we can see, the temperatures in the inner hull are following the scale of the manual calculations. The most critical temperatures are forming above the waterline to the

shipboard and top. The coldest simulated temperature was about -54 °C, and it formed at the local point 18. The most significant differences in the temperatures between the meshes are forming in the inclined top, more specifically in the down corner of the cofferdam (local point 15). The simulated temperatures are coherent with the manual calculations where the temperature under the waterline was calculated to be -6,0 °C, and above the waterline -54,3 °C, when the insulation structure was simplified and radiation was not taken into account.

5.3.4 **Velocity contours**

The forming natural convection can be studied by investigating the forming velocities inside the compartments. At the beginning of simulations, the air is standing inside the compartments, and when the simulation starts to iterate the air inside the compartment starts to move because temperature differences cause density differences between the air particles. Finally, when convergence is achieved, the air finds its balance. After total converging, formed natural convection can be clearly seen. Natural convection streamlines are approximately the same in every mesh. The velocity contour of the situation can be seen in Figure 23. From the temperature point of view, it is crucial that the natural convection is successfully modeled. All the velocity contours can be found in Appendix IV.

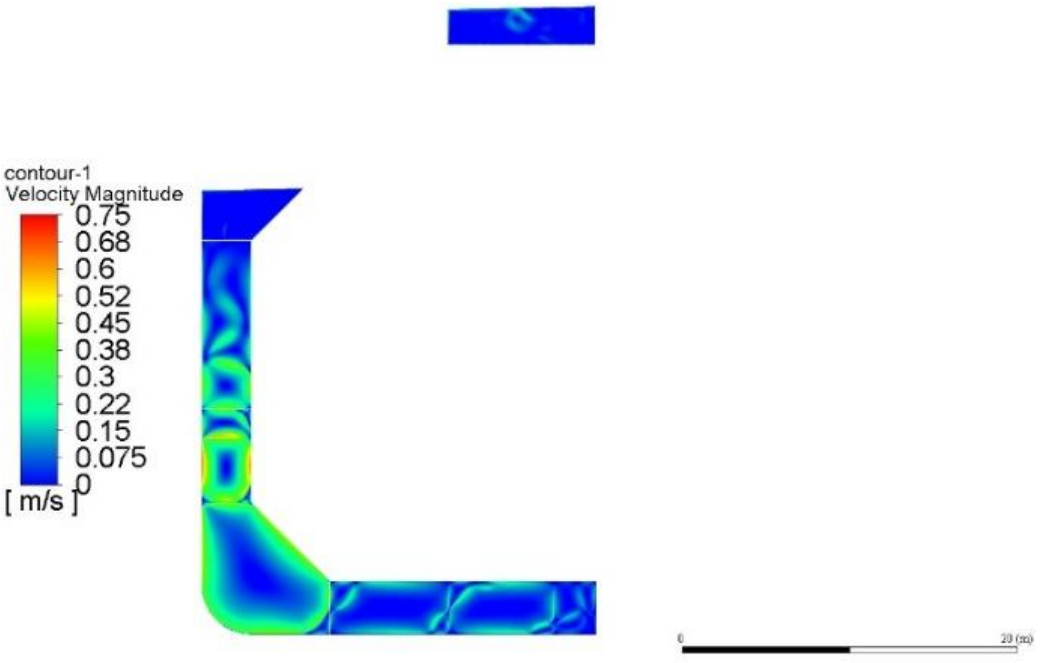

Figure 23 Mesh A velocity contour.

Generally, the highest velocities form in the compartments where the temperature differences are significant between steel plates. For example, if the compartment next to the waterline is compared to the top compartment, the velocities are higher in the waterline compartment. However, a slight difference in flow fields can be seen between the finest mesh, Mesh A, and the coarsest mesh, Mesh C. The streamlines are forming with more accuracy in Mesh A. For example, this can be seen when the long longitudinal compartment is compared between the meshes. The accuracy development can be seen in Figure 24.

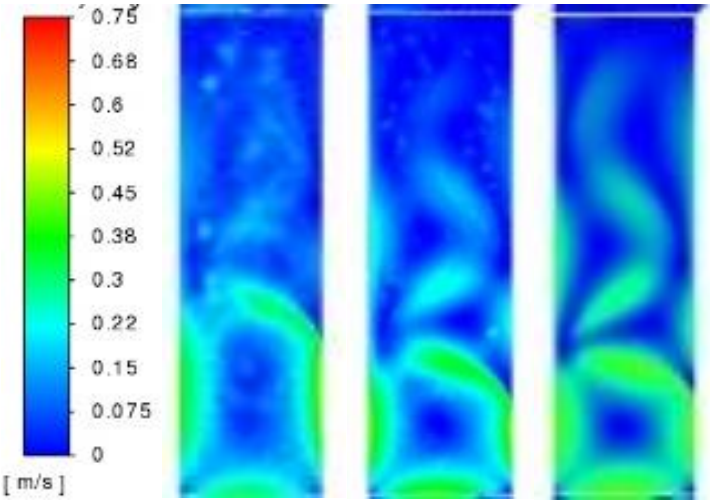

Figure 24 Velocity contours of mesh C, mesh B, and mesh A long compartment.

6 DISCUSS OF THE SIMULATIONS

Preprocessing and solving the models took a significant amount of time. The required computing power was underestimated for doing this thesis work. Especially the meshing process and simulating the densest mesh took a great amount of time. Finding the suitable mesh is an experimental process that is not working on the first try, especially if the designer has not plenty of experiments of meshing in the same kind of applications. Refining and meshing the model over and over again takes time. The denser mesh goes, the more it requires computing power and computing time.

The Ansys student license limitation was underestimated. For that reason, the preliminary plan for the simulation had to be changed. The seawater and ambient air streams have to be deleted from the model because the simulation with them explodes the residuals. The available amount of nodes, 512 000, were not enough for creating enough fine mesh. Different kinds of play moves were tried during the solving process, for example, by reducing the under relaxation factors. But still, the simulation always crashed, and the floating-point was obtained.

In this phase, the water and air streams are easy to simplify by setting the outer steel outer edge temperature to be constant, in above waterline -51°C and below the waterline -1°C. This simplification closes out the CFD analysis of the seawater and ambient air stream velocities effect to the outer hull temperatures. But this part was executed on the 1-D manual model chapter, and the effect was stated to be minor. It can be stated that the drop out of streams was justified. After the simplification was done, the solver could be considered again because when looking at the other scientific research related to free convection modeling, the STT k-ω is not always the best option for the solver (Choi & Kim, 2011, p. 284; Piña-Ortiz, et al., 2014, pp. 271-272). Usage of some other solver could model the free convection better.

The simulations with the final format of the model went well. And the mesh sensitivity analyses did not show significant differences at the end of the results. The biggest difference between the meshes was the computational time. The meshes proceeded as can be assumed, and the mesh C converged fastest because it includes the smallest amount of nodes. Mesh A took the longest time to achieve the converge because it has the highest

number of nodes. The required computational time for achieving full convergence with mesh A was unexpected. After all, the results of all meshes' temperature distributions eventually ended up like expected. The temperature distributions of the steel hull were following to the manual calculations.

From the thermal design point of view, it is unnecessary to look at the velocity fields too specific, but it is still good to look them up, so the heat transfer phenomena inside the compartment are easier to understand. The modeling of forming natural convection has an important key to this kind of heat transfer problem.

7 DEVELOPMENT TARGETS & PLANS

The development plans are related to the model building, calculation power, and Ansys license. At first, the full license of Ansys would make it easier to simulate as a large model as was built on this research. Secondly, the used computing power was abundantly too diminutive for proceeding with this whole process. These two things could make the modeling process more effortless. The real reason why the original model could not achieve the converge can only be guessed because denser mesh could never be tested.

One option could be to split the model into smaller parts, but somehow the splitting would change the entirety of the study. But with good planning and jointing the results could work nicely when the boundaries for the calculation are conceived reasonably. For example, the trunk deck could be left out from the model. The underparts of the model could be modeled as an one part, and the top compartment could be the other part. At the same time, the compartment velocity field and the free convection could be modeled with better accuracy.

Also, gaining more knowledge of the free-convection modeling would absolutely be an advantage for this research topic. At least some iterations should be executed with other solvers than STT k-ω and check if the free-convection could be modeled better.

Using the 3-D model would simplify ambient air and seawater streams in the original model because in 2-D models, the streams had to be modeled against the shipboard as in perpendicular. The perpendicular angle of attack forms a highly turbulent flow next to the shipboard. In the 3-D format, the inlets could be built that they are parallel to the ship structures. This leads to simpler velocity fields, but obviously, more nodes are needed on the mesh when the 3-D model wants to be used.

The models used in this research are not modeling the heat flux phenomenon perfectly because this heat transfer problem is a transient problem for real. The LNG boiling could be modeled example with a simply made inlet for LNG with small velocity so the energy could flow out of the tank somehow in a reasonable way. Another option would be to model the boiling inside the tank. This would require multiphase model usage. However, it can be stated that the steady-state model certainly gives a realistic view of the heat transfer phenomena around the tank.

Many other minor things could be considered again. For example, the steel's roughness affects the velocity field, but the effect to the thermal design point of view is most likely minor. The under relaxation factors modification should be considered more precisely because it might be a key for achieving the converge in the original model. Also, the sloshing inside the tank, sea ice, and waves' effect on the heat transfer phenomena could be investigated. Probably effect of them will be minor if compared to the time to model them. It has to be remembered that using CFD always requires simplification for achieving reasonable results in a reasonable time, especially in the industrial field.

However, the heat transfer problem of this thesis could be modeled successfully with CFD, and the results are as expected. Even the CFD modeling part seemed challenging at some phases. At finally, reasonable results were achieved, and the made simplifications worked nicely as well.

8 CONCLUSIONS

It can be stated that IMO is the primary detective body that drives the whole ship industry's safety issues by legislating international regulations. These regulations create the main principles for the ship's operation and design, but practically they do not guide the designer, they rather only set them the baselines. The classification societies ensure that ship design and construction are fulfilling the IMO's requirements. The classification societies establish rules, regulations, and guidelines. The more specific documents are helping to achieve the requirements from the ship design point of view.

The LNG carrier hull thermal design preliminary boundaries could be achieved with manual calculations. It proved that radiation, contact resistances, and outside convection effectiveness in the steel grade design are almost negligible from the basic design point of view. This study stated that 1-D calculation is a simple way to execute when the basic theory of heat transfer is understood, and the calculation results can be assumed to be reliable. 1-D manual calculations are determining the temperature as there is no heat flow in y- or z-direction. This can be seen in a way that the manual calculation above the waterline determines the coldest temperature in the structure that should be formed to the whole model if all thermal bridges have not been taken into account. On the other hand, the manual calculations describe the steel structure temperatures below the waterline favorable way, and the results determine the warmest temperatures in the steel structure. Practically all formed temperatures in steel structure settle between these values.

For achieving more realistic results from the whole entirety; the multidimensional models should be executed. Determining multidimensional manual models are ponderous, and for that reason, the program-based solution should be considered. During the CFD modeling process, it can be stated that modeling this type of heat transfer case is not as simple as someone would initially think. Firstly, modeling the problem as a one-piece is challenging with the Ansys student license's node limitation. When the built CFD model consists of seawater and air streams, the simulation will face convergence problems.

When the CFD model is simplified out of ambient streams, it requires different boundaries for the calculations. These boundaries can be taken from manual calculations. When the simulation proceeds to the end and the simulation achieves convergence, the

flow inside the compartment starts to stabilize. The simulation of all three different resolution meshes achieved reasonable results from the temperature distribution point of view. Also, there were no significant differences in the temperature distributions of the inner hull between the meshes. However, the finest mesh, mesh A, simulated the forming natural convection in the compartments with the best accuracy. Based on that, it can be stated that certainly fine mesh is recommended because if the natural convection could be modeled with good accuracy, the results of temperature distribution are also more accurate.

The coldest simulated temperatures formed shipboard above the water line and the top of the tank. The coldest simulated temperature was -54,1 °C. The warmest temperatures in the inner hull were simulated in the ship bottom, as was expected. The warmest simulated temperature in the inner hull was -6,4 °C. The simulated results were coherent with manually calculated temperatures. The manually calculated coldest temperature was -54,3 °C, and the calculated warmest temperature was -6,0 °C. It can be stated that based on the simulations, the steel grade selection of the designed ship could be executed with CFD with certainly good reliability.

The next step would be to focus on the CCS's damage scenario. During the arctic voyages, if the ship is facing any breakage in the insulation structure, the ship hull structure will face severe issues. This happens because the ship is operating in a cold climate, so the impact strength limit of hull steel plates can be potentially obtained. Additionally, the nearest harbor might be far away. In any scenario, this is not permissible. Solving the problem and studying how to avoid critical temperatures during the leakage should be investigated in the future.

BIBLIOGRAPHY

American Bureau of Shipping B, n.d. *Low Temperature Operations - Guidance for Arctic Shipping.* Houston: American Bureau of Shipping.

American Bureau of shipping, ., 2019. *Thermal analysis of vessels with tanks for liguefied gas.* Texas TX: American Bureau of shipping.

Anderson Jr., J. D., Degroote, J., Degrez, D., Dick, E., Grundman, R., & Vienrendeels, J., 2009. *Computational Fluid Dynamics.* 3rd ed. Berlin: Springer.

ANSYS, 2013. *ANSYS Fluent User's Guide.* Canonsburg: ANSYS, Inc..

Babu, K. N., 2015. *Thermal Contact Resistance: Experiments and Simulation.*. Gothenburg: Chalmers University og Technology - Master's thesis in Automotive Engineerign..

Bagaev, D. V., Syraleva, M. N. & Kudinovich, I. V., 2020. Comperative analysis of energy efficiency of ballast tank anti-freezing systems. *Journal of Physics,* Conference Series, 1683(2)(http://dx.doi.org.ezproxy.cc.lut.fi/10.1088/1742-6596/1683/2/022023), pp. 1-10.

Boz, Z., Erdogdu, F. & Tutar, M., 2014. Effects of mesh refinement, time step size and numerical scheme on the computational modeling of temperature evolution during natural-convection heating. *Journal of Food Engineering,* Volume 123, pp. 8-16.

Choi, S.-K. & Kim, S.-O., 2011. Turbulence modeling of natural convection in enclosures: A review. *Journal of Mechanical Science and Technology,* 26(1), pp. 283-297.

Choi, S. W., Roh, J. U., Kim, M. S. & Lee, W. I., 2012. Analysis of two main LNG CCS (cargo containment system) insulation boxes for. *Applied Ocean Research,* Volume 37, pp. 72-89.

Ding, S.-f., Tang, W.-y. & Zhang, S.-k., 2010. *Research on Temperature Field and Thermal Stress of Liguefied Natural Gas Carrier with Incomplete Insulation.*. Shanghai: Shanghai Jiaotong University and Springer-Verlag Berlin Heidelberg.

DNV·GL, 2015. *Winterization for cold climate operations.* Oslo: DNV GL Group.

Grassi, W., 2018. *Heat Pumps Fundamentals and Applications.* 1st ed. Pisa: Springer International Publishing.

GTT Training Ltd., 2015. *GGT Membrane Cargo Containment Systems.* [Online] Available at: https://www.onthemosway.eu/wp-content/uploads/2015/06/GTT-Training-Membrane-Tanks.compressed.pdf
[Accessed 1 June 2021].

GTT, 2020a. *Mark III systems.* [Online] Available at: https://www.gtt.fr/en/technologies/markiii-systems [Accessed 20 January 2021].

GTT, 2020b. *NO96 systems.* [Online] Available at: https://www.gtt.fr/en/technologies/no96-systems [Accessed 20 January 2021].

IACS, 2021. *International Association of Classification Societies.* [Online] Available at: http://www.iacs.org.uk/ [Accessed 1 February 2021].

IMO, 2007. *FSA - Liquefied Natural Gas (LNG) Carriers Details of the Formal Safety Assessment.* Denmark: IMO - Maritime Safety Committee.

IMO, 2014. *Amendments to the international code for the construction and equipment of ships carrying liquefied gases in bulk. IGC CODE. MSC.370(93).* London: IMO.

Incropera, F. P., Dewitt, D. P., Bergman, T. L. & Lavine, A. S., 2007. *Fundamentals of Heat and Mass Transfer.* 6th ed. New Jersey: John Wiley & Sons, Inc.

Jameson, A., 2012. *Computational Fluid Dynamics Past, Present and Future.* California: Department of Aeronautics & Astronautics.

Joeng, H. & Shim, W. J., 2017. CALCULATION OF BOIL-OFF GAS (BOG) GENERATION OF KC-1 MEMBRANE LNG TANK WITH HIGH DENSITY RIGID POLYURETHANE FOAM BY NUMERICAL ANALYSIS. *Polish maritime research,* 24, no.1(DOI: https://doi.org/10.1515/pomr-2017-0012), pp. 100-114.

Kendrick, A. & Daley, D. C., 2011. *Structural Challenges Faced of Arctic Ships.* Kanata: Ship Structure Committee.

Korean Register, 2020. *Guidance of Heat Transfer Analysis for Ships Carrying Liquefied Gases in Bulk/Ships Using Liqueifed Gases as Fuels.*. Busan: Korean Register.

Lloyd's Register, 2016. *Guidelines for requirements of thermal analysis for the hull structure of ships carrying liquefied gases in bulk.* London: Lloyd's Register Group.

Mokhatab, S., Mak, J. Y., Valappil, J. V. & Wood, D. A., 2013. *Handbook of Liquefied Natural Gas.* 1st ed. Saint Louis: Elsevier Science & Technology.

Pastausiak, T., 2016. *The Northern Sea Route as a Shippin Lane.* 1st ed. Switzerland: Springer International Publishing.

Piña-Ortiz, A., Hinojosa, J. & Maytorena, V., 2014. Test of turbulence models for natural convection in an open cubic tilted cavity. *International Communications in Heat and Mass Transfer,* Volume 57, pp. 264-273.

Qu, Y., Ibrahmina, N., Xiachun, X., Privat, R. & Jauber, J., 2019. A thermal and thermodynamic code for the computation of Boil-Off Gas - Industrial applications of LNG carrier. *Gyrogenics*, Volume 99, pp. 105-113.

Räsänen, P., 2000. *Laivatekniikka - Modernin laivanrakennuksen käsikirja.* 2nd ed. Jyväskylä: Gummerus Kirjapaino Oy.

Simscale, 2021. *K-Omega and K-Omega SST.* [Online] Available at: https://www.simscale.com/docs/simulation-setup/global-settings/k-omega-sst/
[Accessed 1 June 2021].

Stephan, P., Kabelac, S., Kind, M., Martin, H., Mewes, D. & Schaber, K., 2010. *VDI Heat Atlas.* 2nd ed. Düsseldorf: VDI-GVC.

Sung, W. C., Han, S. K. & Woo, L. L., 2016. Analysis of leaked LNG flow and consequent thermal effect for safety in LNG cargo containment system. *Ocean Engineering,* Volume 113, pp. 276-294.

Tu, J., Yeoh, G.-H. & Chaoqun , L., 2018. *Computational Fluid dynamics - A Practical Approach.* 3rd ed. Oxford & Cambridge: Elsevier Ltd.

USCG, 2015. America's Energy Renaissance. *PROCEEDINGS of the Marine Safety and Security Council. Vol 72, NO3*, Fall.

Vepsäläinen, A., Pitkänen, J. & Hyppänen, T., 2012. *Fundamentals of Heat Transfer.* Lappeenranta: Lappeenranta University of Technology. Faculty of Technology. LUT Energy..

White, F. M., 2011. *Fluid Mechanics.* 7th ed. New York: McGraw-Hill.

APPENDIX I

Table 6.2 of the IGC Code

PLATES, SECTIONS AND FORGINGS [See note1] FOR CARGO TANKS, SECONDARY BARRIERS AND PROCESS PRESSURE VESSELS FOR DESIGN TEMPERATURES BELOW 0°C AND DOWN TO -55°C Maximum thickness 25 mm [See note 2]					
CHEMICAL COMPOSITION AND HEAT TREATMENT					
◆ Carbon-manganese steel					
◆ Fully killed, aluminium treated fine grain steel					
◆ Chemical composition (ladle analysis)					
C	Mn	Si	S	P	
0.16%max [See note 3]	0.7-1.60%	0.1-0.50%	0.025% max	0.025% max	
Optional additions: Alloys and grain refining elements may be generally in accordance with the following:					
Ni	Cr	Mo	Cu	Nb	V
0.8% max	0.25% max	0.08% max	0.35% max	0.05% max	0.1% max
Al content total 0.02% min (Acid soluble 0.015% min)					
◆ Normalized, or quenched and tempered [See note 4]					
TENSILE AND TOUGHNESS (IMPACT) TEST REQUIREMENTS					
Sampling frequency					
◆ Plates	Each "piece" to be tested				
◆ Sections and forgings	Each "batch" to be tested				
Mechanical properties					
◆ Tensile properties	Specified minimum yield stress not to exceed 410 N/mm^2 [See note 5]				
Toughness (Charpy V-notch test)					
◆ Plates	Transverse test pieces. Minimum average energy value (KV) 27J				
◆ Sections and forgings	Longitudinal test pieces. Minimum average energy (KV) 41J				
◆ Test temperature	5°C below the design temperature or -20°C, whichever is lower				

Notes

1 The Charpy V-notch and chemistry requirements for forgings may be specially considered by the Administration.

2 For material thickness of more than 25 mm, Charpy V-notch tests shall be conducted as follows:

Material thickness (mm)	Test temperature (°C)
25 < t ≤ 30	10°C below design temperature or -20°C, whichever is lower
30 < t ≤ 35	15°C below design temperature or -20°C, whichever is lower
35 < t ≤ 40	20°C below design temperature
40 < t	Temperature approved by the Administration or recognized organization acting on its behalf

The impact energy value shall be in accordance with the table for the applicable type of test specimen.

Materials for tanks and parts of tanks which are completely thermally stress relieved after welding may be tested at a temperature 5°C below design temperature or -20°C, whichever is lower.

For thermally stress relieved reinforcements and other fittings, the test temperature shall be the same as that required for the adjacent tank-shell thickness.

3 By special agreement with the Administration, the carbon content may be increased to 0.18% maximum, provided the design temperature is not lower than -40°C.

4 A controlled rolling procedure or TMCP may be used as an alternative.

5 Materials with specified minimum yield stress exceeding 410 N/mm^2 may be approved by the Administration or recognized organization acting on its behalf. For these materials, particular attention shall be given to the hardness of the welded and heat affected zones.

Guidance:

For materials exceeding 25 mm in thickness for which the test temperature is -60°C or lower, the application of specially treated steels or steels in accordance with table 6.3 may be necessary.

APPENDIX II

Table 6.3 of the IGC code

PLATES, SECTIONS AND FORGINGS See note 1 FOR CARGO TANKS, SECONDARY BARRIERS AND PROCESS PRESSURE VESSELS FOR DESIGN TEMPERATURES BELOW -55°C AND DOWN TO -165°C See note 2 Maximum thickness 25 mm See notes 3 and 4		
Minimum design temperature (°C)	Chemical composition See note 5 and heat treatment	Impact test temperature (°C)
-60	1.5% nickel steel – normalized or normalized and tempered or quenched and tempered or TMCP See note 6	-65
-65	2.25% nickel steel – normalized or normalized and tempered or quenched and tempered or TMCP See notes 6 and 7	-70
-90	3.5% nickel steel – normalized or normalized and tempered or quenched and tempered or TMCP See notes 6 and 7	-95
-105	5% nickel steel – normalized or normalized and tempered or quenched and tempered See notes 6, 7 and 8	-110
-165	9% nickel steel – double normalized and tempered or quenched and tempered See note 6	-196
-165	Austenitic steels, such as types 304, 304L, 316, 316L, 321 and 347 solution treated See note 9	-196
-165	Aluminium alloys; such as type 5083 annealed	Not required
-165	Austenitic Fe-Ni alloy (36% nickel). Heat treatment as agreed	Not required
TENSILE AND TOUGHNESS (IMPACT) TEST REQUIREMENTS		
Sampling frequency		
◆ Plates	Each "piece" to be tested	
◆ Sections and forgings	Each "batch" to be tested	
Toughness (Charpy V-notch test)		
◆ Plates	Transverse test pieces. Minimum average energy value (KV) 27J	
◆ Sections and forgings	Longitudinal test pieces. Minimum average energy (KV) 41J	

Notes

1 The impact test required for forgings used in critical applications shall be subject to special consideration by the Administration.

2 The requirements for design temperatures below -165°C shall be specially agreed with the Administration.

3 For materials 1.5% Ni, 2.25% Ni, 3.5% Ni and 5% Ni, with thicknesses greater than 25 mm, the impact tests shall be conducted as follows:

Material thickness (mm)	Test temperature (°C)
$25 < t \leq 30$	10°C below design temperature
$30 < t \leq 35$	15°C below design temperature
$35 < t \leq 40$	20°C below design temperature

	The energy value shall be in accordance with the table for the applicable type of test specimen. For material thickness of more than 40 mm, the Charpy V-notch values shall be specially considered.
4	For 9% Ni steels, austenitic stainless steels and aluminium alloys, thickness greater than 25 mm may be used.
5	The chemical composition limits shall be in accordance with recognized standards.
6	TMCP nickel steels will be subject to acceptance by the Administration.
7	A lower minimum design temperature for quenched and tempered steels may be specially agreed with the Administration.
8	A specially heat treated 5% nickel steel, for example triple heat treated 5% nickel steel, may be used down to -165°C, provided that the impact tests are carried out at -196°C.
9	The impact test may be omitted, subject to agreement with the Administration.

APPENDIX III

Temperature contours

Mesh A

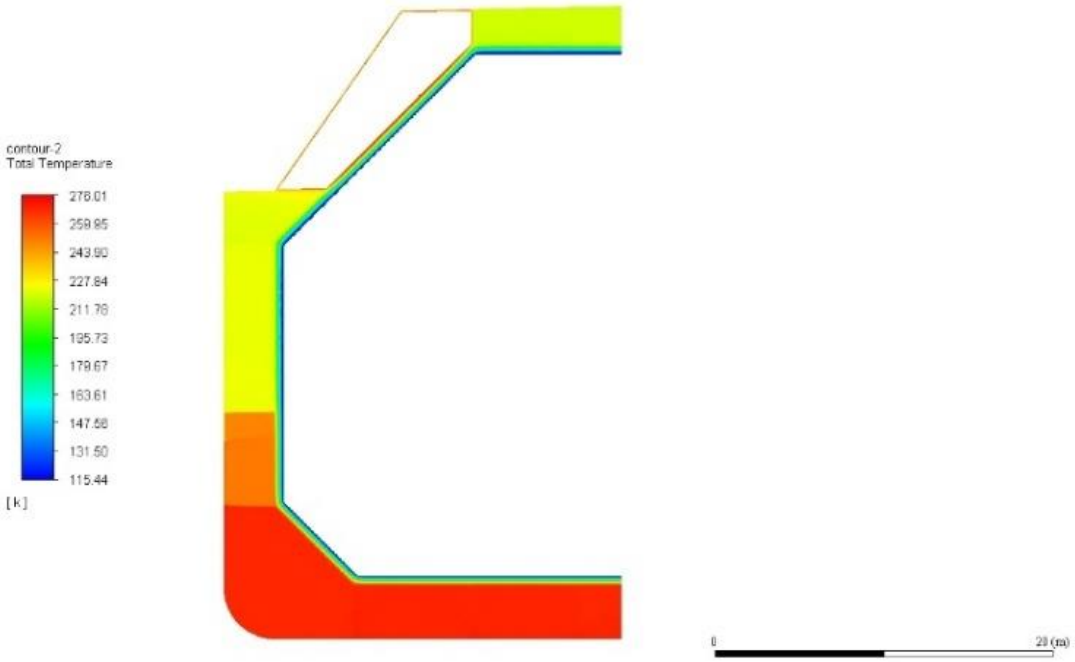

Mesh B

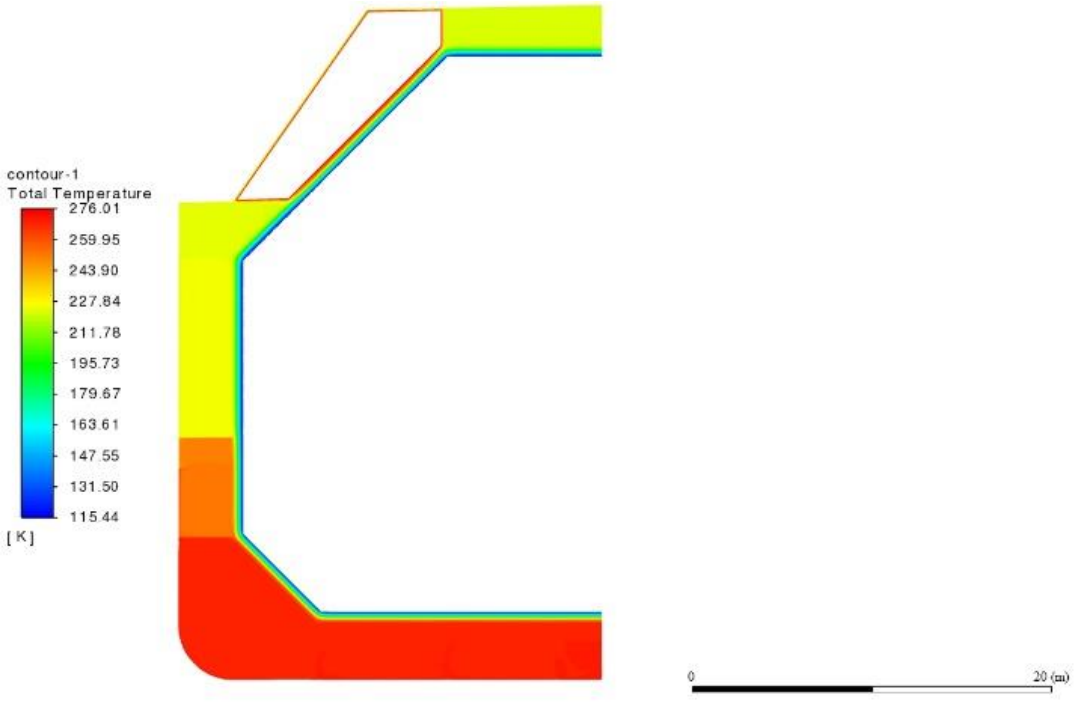

Mesh C

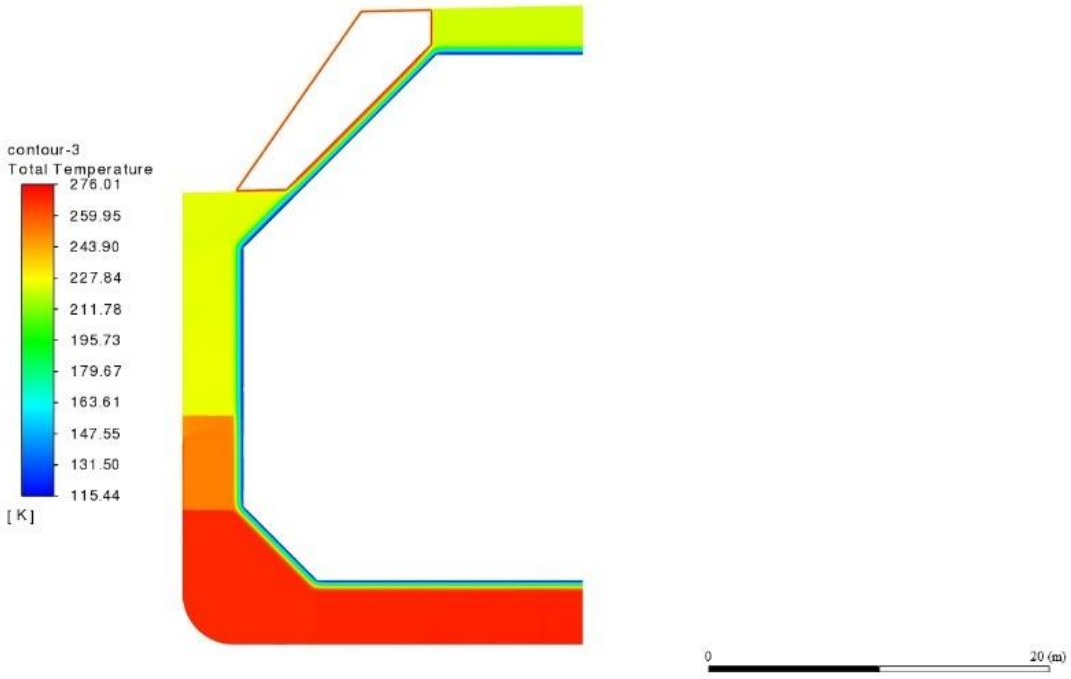
contour-3
Total Temperature
276.01
259.95
243.90
227.84
211.78
195.73
179.67
163.61
147.55
131.50
115.44
[K]
0
20 (m)

APPENDIX IV

Velocity contours

Mesh A

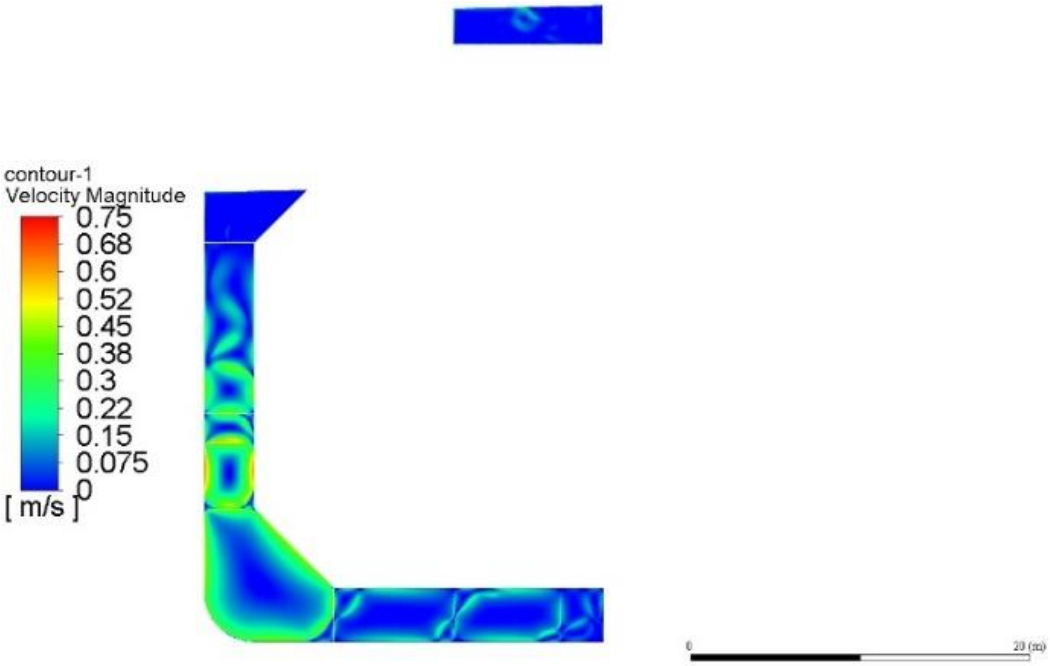

Mesh B

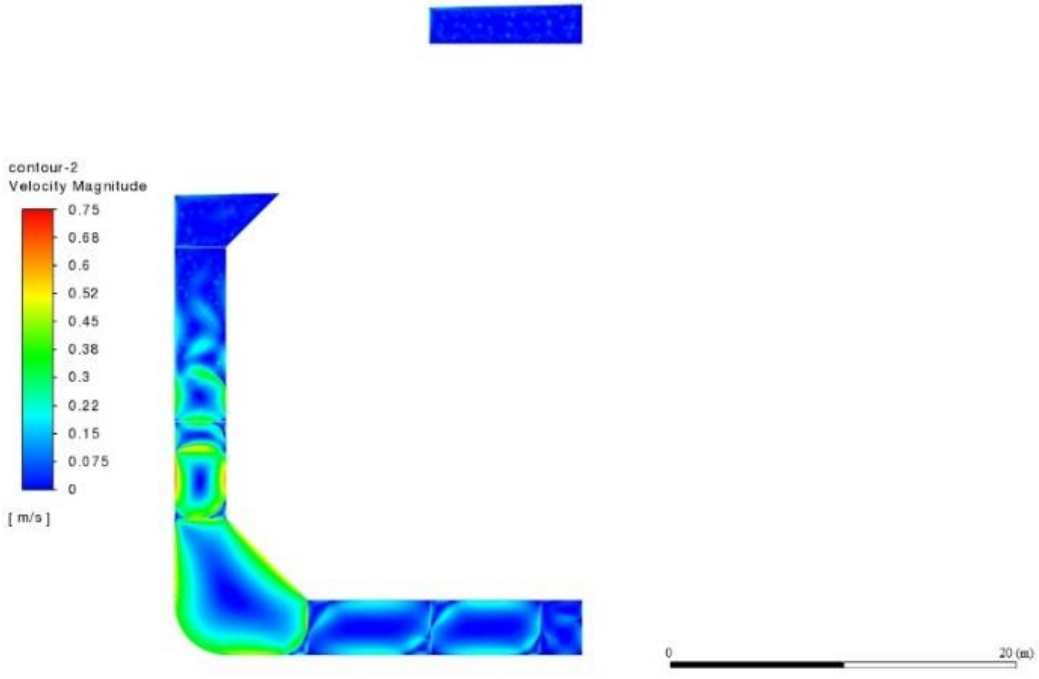

Mesh C

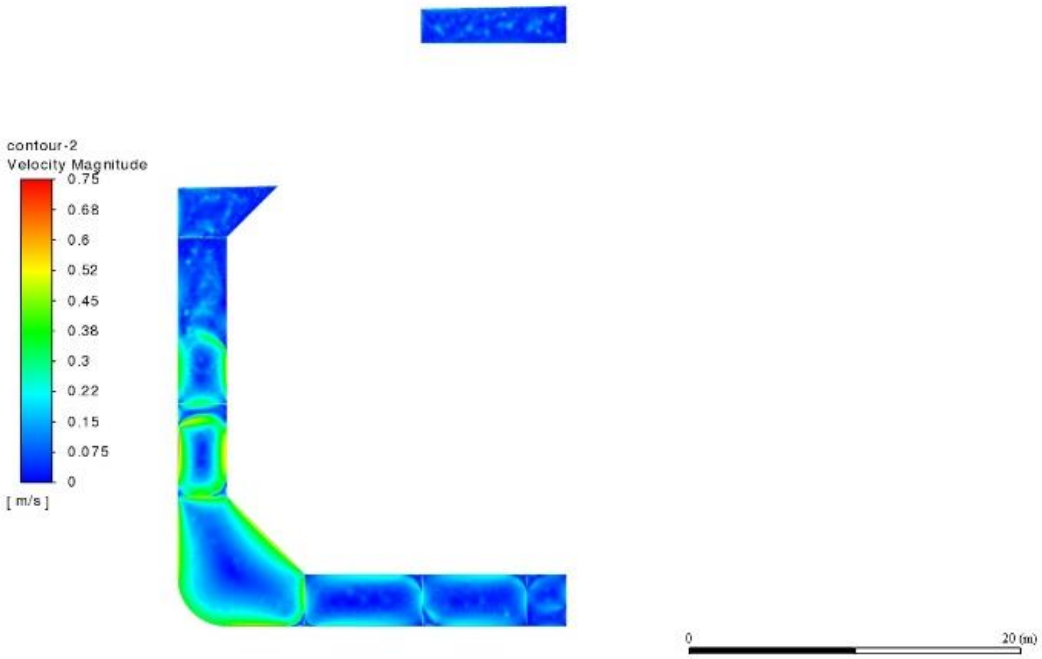
contour-2
Velocity Magnitude
0.75
0.68
0.6
0.52
0.45
0.38
0.3
0.22
0.15
0.075
0
[m/s]
0
20 (m)